ARL-TR-9032 ● AUG 2020

DEVCOM ARMY RESEARCH LABORATORY

An Opposed-Flow Diffusion Flame Simulation-Based Implementation of the Trial Mechanism Method for Chemical Kinetics Mechanism Reduction: Application to the San Diego Mechanism for HTPB-Air Combustion Modeling

by Michael McQuaid

NOTICES

Disclaimers

The findings in this report are not to be construed as an official Department of the Army position unless so designated by other authorized documents.

Citation of manufacturer's or trade names does not constitute an official endorsement or approval of the use thereof.

Destroy this report when it is no longer needed. Do not return it to the originator.

ARL-TR-9032 ● AUG 2020

An Opposed-Flow Diffusion Flame Simulation-Based Implementation of the Trial Mechanism Method for Chemical Kinetics Mechanism Reduction: Application to the San Diego Mechanism for HTPB-Air Combustion Modeling

Michael McQuaid
Weapons and Materials Research Directorate, CCDC Army Research Laboratory

REPORT DOCUMENTATION PAGE

Form Approved
OMB No. 0704-0188

1. REPORT DATE *(DD-MM-YYYY)*	2. REPORT TYPE	3. DATES COVERED (From - To)
August 2020	Technical Report	November 2019–June 2020

4. TITLE AND SUBTITLE
An Opposed-Flow Diffusion Flame Simulation-Based Implementation of the Trial Mechanism Method for Chemical Kinetics Mechanism Reduction: Application to the San Diego Mechanism for HTPB-Air Combustion Modeling

5a. CONTRACT NUMBER

5b. GRANT NUMBER

5c. PROGRAM ELEMENT NUMBER

6. AUTHOR(S)
Michael McQuaid

5d. PROJECT NUMBER

5e. TASK NUMBER

5f. WORK UNIT NUMBER

7. PERFORMING ORGANIZATION NAME(S) AND ADDRESS(ES)
CCDC Army Research Laboratory
ATTN: FCDD-RLW-LD
Aberdeen Proving Ground, MD 21005

8. PERFORMING ORGANIZATION REPORT NUMBER
ARL-TR-9032

9. SPONSORING/MONITORING AGENCY NAME(S) AND ADDRESS(ES)

10. SPONSOR/MONITOR'S ACRONYM(S)

11. SPONSOR/MONITOR'S REPORT NUMBER(S)

12. DISTRIBUTION/AVAILABILITY STATEMENT
Approved for public release; distribution is unlimited.

13. SUPPLEMENTARY NOTES
ORCID ID: Michael McQuaid, 0000-0001-5523-7468

14. ABSTRACT
Seeking more effective means for producing skeletal finite-rate chemical-kinetics mechanisms for modeling propulsion systems whose dynamics are strongly coupled to non-premixed combustion processes, the author developed a variation of the trial mechanism method (TMM) for mechanism reduction that involved comparing solutions to quasi-1-dimensional opposed-flow diffusion flame (OFDF) problems. To evaluate this variation's cost and performance, it was applied to create from the 323 reaction-67 species San Diego (SD) mechanism skeletal mechanisms for simulating the combustion of hydroxyl-terminated polybutadiene (HTPB)-air in an opposed-flow burner. The results were encouraging. A candidate comprising 88 reactions and involving 38 species was found able to mimic well the SD mechanism throughout the parameter space of interest. Moreover, though more difficult to set up and apply than TMMs with screening protocols that compare solutions to homogeneous reactor problems, the overall costs of the two approaches proved to be competitive when the cost to vet candidates was included. Considerations in prescribing an OFDF-TMM's screening protocol are discussed. Issues in developing and applying OFDF-TMMs for the reduction of larger mechanisms were anticipated, and means for addressing them proposed.

15. SUBJECT TERMS
chemical kinetics, combustion, diffusion flame, regression rates, solid-fuel ramjet

16. SECURITY CLASSIFICATION OF:			17. LIMITATION OF ABSTRACT	18. NUMBER OF PAGES	19a. NAME OF RESPONSIBLE PERSON
a. REPORT	b. ABSTRACT	c. THIS PAGE			Michael McQuaid
Unclassified	Unclassified	Unclassified	UU	78	19b. TELEPHONE NUMBER (Include area code) (410)-278-6185

Contents

List of Figures

List of Tables

Acknowledgments

I am grateful to Dr Anthony Kotlar (US Army Combat Capabilities Development Command [CCDC] Army Research Laboratory [ARL], retired) for sharing his insights into the application of thermodynamic principles for the prediction of propulsion system performance and entrusting me with his invention. It was a spark of genius that has greatly contributed to CCDC Army Research Laboratory's capacity to develop finite-rate chemical kinetics mechanisms for propulsion system modeling.

Funding for this study was provided by ARL's Long-Range Distributed and Collaborative Engagements mission program and by the Office of Naval Research. The reduction protocols were run on a DoD Shared Resource Center High Performance Computing (DSRC-HPC) platform at ARL, Aberdeen Proving Ground, Maryland.

1. Introduction

As discussed in two previous reports (Chen and McQuaid 2020; McQuaid 2020), Propulsion Science Branch (PSB) researchers at the US Army Combat Capabilities Development Command (CCDC) Amy Research Laboratory (ARL) are developing and validating "detailed" finite-rate chemical kinetics mechanisms that can be used as a basis for simulating reacting flows in solid-fuel ramjet (SFRJ) combustors. (Detailed finite-rate chemical kinetics mechanisms are networks comprising molecular and/or atomic species connected by elementary reactions.) SFRJs are air-breathing engines in which the compression of air that is needed to raise its temperature and pressure to values that can sustain the fuel's combustion is provided by the projectile's forward motion (alone). Offering a good balance of (mechanical) simplicity, (relatively) low cost, specific impulse, and speed, an SFRJ also will not respond violently to threats of concern, making it an insensitive munitions technology as well. However, the technical challenges that must be overcome before SFRJs can be fielded are considerable. Physics-based computational fluid dynamics (CFD) models have the potential to accelerate their development by providing insights useful in identifying and resolving issues at "off-design" conditions (Krishnan and George 1998). Driven largely by thermochemical (reaction) kinetics, the accuracy and reliability of a model's predictions depend critically on its chemical kinetics mechanism's capacity to simulate reaction dynamics under such conditions. The development of the mechanism reduction technique summarized in this report was prompted by this matter.

In conjunction with efforts to develop CFD models for simulating reacting flows in SFRJ combustors fueled with hydroxyl-terminated polybutadiene (HTPB), PSB has assembled a comprehensive detailed mechanism for modeling its ignition and combustion with air (Chen and McQuaid 2009, 2010, 2011, 2015, 2020). Including elementary reactions for decomposing a relatively large hydrocarbon ($C_{20}H_{32}$) with a molecular structure that is nominally similar to HTPB type R45M polymer chains, it comprises more than 2750 reactions and more than 800 species. As such, those numbers far exceed those that can compose a thermochemical kinetics submodel for a multidimensional, temporally transient SFRJ combustor model. Imposed by the computational costs they engender, limits derive from the fact that species conservation requires that the set of governing equations representing the dynamics include a partial differential equation (PDE) for every species in the mechanism, and each reaction adds a source term to each PDE. Dictated by available computing

power and the efficiency with which a CFD model can avail itself of that power, current limits are (approximately) ≤120 reactions and ≤100 species. (They have increased somewhat over the years.)

Cognizant of these limits at the outset of the $C_{20}H_{32}$-air mechanism's development, we anticipated deriving "skeletal" mechanisms with the capacity to mimic the "full" mechanism under conditions established in an SFRJ combustor during flight. (A skeletal mechanism comprises a subset of the full mechanism's reactions and species.) Since 2004, PSB has accomplished similar objectives via a technique that its inventor and original developer—Dr Anthony Kotlar (ARL, retired)—called the "trial mechanism method" (TMM) (Kotlar 2010). Discussed in more detail in section 4.1, it predicates the elimination of reactions from a full mechanism based on comparing full- and trial-mechanism-based solutions for combustion problems that are relevant to, but (significantly) less expensive to solve than, those of specific interest. Species are eliminated when all reactions involving them are eliminated.

To date, the problem type whose solutions have been analyzed for that purpose has been the time evolution of a homogeneous reacting gas mixture. (Such solutions will also be referred to herein as homogeneous reactor [HR] simulations.) Applied to the $C_{20}H_{32}$-air mechanism to generate skeletal mechanisms for modeling dynamics in a connected-pipe SFRJ combustor, it produced a 128 reaction-106 species candidate whose validity for the application was evaluated. Employed as the basis for steady quasi-one-dimensional (1-D) opposed-flow diffusion flame (OFDF) simulations considered relevant to the application, it was found able to reproduce key features of simulations produced with larger skeletal mechanisms (Chen and McQuaid 2020). Therefore, it was transitioned for incorporation into an SFRJ combustor model (Nusca et al. 2019) where it will be further evaluated.

That achievement notwithstanding, the potential for an HR-TMM to produce skeletal mechanisms that will mimic well a full one's capacity to represent the thermochemical kinetics associated with the combustion of a solid fuel (grain) and a gaseous oxidizer as takes place in SFRJ combustors is somewhat speculative. Adjacent to the solid–gas interface, the fuel and oxidizer components are not (necessarily) well mixed, and it cannot be expected that the chemical composition's spatial/temporal evolution will be mirrored in an HR simulation. Therefore, the reactions and species that control the dynamics could be different in the two cases. Moreover, molecular transport/diffusion may also be germane, but it does not play a role in HR simulations. Therefore, there could be reactions and species retained that are unnecessary for modeling the dynamics of interest. In addition, there may be some reactions and species whose inclusion would improve its capacity to mimic the full mechanism within the parameter space of interest. Given that the size of smallest skeletal mechanism derived from the $C_{20}H_{32}$-air mechanism for the

application is already at the current limit that can be used in an SFRJ combustor model and the parameter space of the screening protocol that produced it only encompassed "on-design" conditions, establishing screening protocols that are more efficient will be necessary to produce viable candidates for modeling off-design conditions.

In view of the TMM concept's generality, an approach with the potential to address such issues has long been postulated; namely, replace the screening protocol's HR simulations with a canonical non-premixed problem type, such as steady 1-D OFDF simulations. Moreover, since the TMM's incarnation, the capacity to set up and solve such problems has been available in the form of a pre-commercial version of the CHEMKIN program OPPDIF (Lutz et al. 1997). However, based on my early experience with the CHEMKIN program for modeling 1-D premixed flames—namely PREMIX (Kee et al. 1985), which is a close cousin of OPPDIF—I did not think an OFDF-TMM would be computationally feasible. As then being implemented for propulsion system applications (in the early 2010s), HR-TMM-based efforts were already requiring resources that were near practical limits. (Concerned more about timeliness and efficiency than computational cost, I wanted screening protocols to complete within the maximum wall time [168 h, 1 week] permitted for standard jobs on DoD Shared Resource Center High Performance Computing [DSRC-HPC] platforms.) Being directly related to the number of reactions in the mechanism, the number of protocol-prescribed problems, and the time required to solve those problems, the overall wall times for HR-TMM jobs were approaching 168 h when screening protocols included HR simulations that (individually) were taking less than 10 s to perform and evaluate. My experience with PREMIX indicated that relevant OPPDIF problems would take many minutes to solve, and therefore would be an impractical basis for a protocol.

My general pessimism about the potential for an OFDF-TMM to be practical lessened in the course of developing a program to predict the burning rates of monopropellants and explosives based on the CYCLOPS framework (Miller and Anderson 2000, 2004). That effort was motivated by my struggle to understand and apply Dr Martin Miller's (original) CYCLOPS program. Predicated on adjusting the inlet temperature (T^0) and mass flow rate ($\dot{M}$) of a PREMIX problem such that an energy-flux boundary condition at the ($x = 0$) inlet was met (see Section 4.4), Dr Miller's program started each new PREMIX problem (corresponding to an adjustment in T^0 and/or $\dot{M}$) "from scratch". That is, a coarse (6-point) grid was specified and initial values for state variables at each point were estimated using methods PREMIX made available for that purpose. Becoming impatient with the tens of minutes it was taking to produce solutions in this manner, I decided to investigate Kee et al.'s statement that "It often saves computer time to begin a

computation for a given flame by starting with the solution of another flame that is in some sense related" (Kee et al. 1985). Since the changes being made to T^0 and $\dot{M}$ were small, the successive problems were obviously related to one another. Therefore, I wrote my own CYCLOPS-based burning rate predictor program and incorporated coding such that the solution to the most recently solved problem established initial estimates for the next problem. Very unexpectedly, I found that Kee et al.'s comment was a gross understatement (at least with respect to this application). The succeeding problems were solved in a couple of seconds.

Presuming the run-times of OPPDIF-based OFDF simulations would be similar, I developed an OFDF-TMM (program) whose screening protocol involved comparing simulation parameter values that were analogous to those compared in PSB-developed HR-TMMs. To beta test the program, I employed it to reduce a 20 reaction-9 species mechanism for modeling H_2–O_2 combustion that was provided for an example problem in the OPPDIF manual (Lutz et al. 1997). Screening trial-mechanism-based solutions for several variations of the example problem, it produced skeletal mechanisms that were comparable in size to those produced with an HR-TMM (McQuaid 2013b), and the temperature (T) and heat-release rate ($\dot{q}$) versus distance (d) profiles produced with the smallest (8 reaction-8 species) candidate were in good agreement with those produced with the full mechanism.

That success notwithstanding, the reduction of larger mechanisms with an OFDF-TMM was (and remains) a daunting prospect. In particular, to get started, a solution to a relevant OFDF problem has to be obtained from scratch, and that can be extremely difficult when the mechanism is very large. Required resources (primarily labor) have the potential to be considerable, and a payoff is not guaranteed. Therefore, lacking a compelling need (e.g., candidates produced with an HR-TMM had significant shortcomings), I did not use it for applications where it may have been more effective than an HR-TMM (e.g., see McQuaid et al. [2019]).

This report summarizes my first attempt to develop and apply an OFDF-TMM for a "real" application. That application is the creation of skeletal mechanisms that can be employed to model the combustion of HTPB in an opposed-flow burner. Funded (in part) by the Office of Naval Research, it was undertaken in conjunction with a collaborative project involving Naval Research Laboratory, Naval Air Warfare Center, and Naval Sea Warfare Center researchers to elucidate mechanisms of HTPB–air ignition and combustion in SFRJ combustors. In the project, flames produced by combusting (solid) HTPB and (gaseous) N_2–O_2 mixtures are to be probed with various spectroscopic techniques, and those

experiments are to be modeled. PSB researchers are responsible for developing detailed finite-rate chemical kinetics mechanisms to represent the gas phase's thermochemical kinetics.

Pertaining to that aspect of the project, there was interest within the team in assuming the nascent product of HTPB's pyrolysis was 1,3-butadiene (C_4H_6) and modeling its air-oxidized combustion chemistry with a general, open-source chemical kinetics mechanism that was developed by the University of California San Diego Combustion Research Group. Called by its developers "the San Diego (SD) mechanism", when the effort summarized herein commenced, it comprised five separate modules and a mechanism suitable for modeling C_4H_6–air combustion could be constructed by combining three of them. With (exact) duplicate reactions eliminated, the combination comprised constants for computing the rates of 323 elementary reactions and thermochemical and transport properties for 67 species.

Unlike CCDC Army Research Laboratory's $C_{20}H_{32}$–air mechanism, the full (323 reaction-67 species) SD mechanism is readily usable by steady quasi-1-D OFDF models, and they have the potential to reasonably simulate the proposed experiments. Those models' ability to reproduce results derived from the experiments will therefore justify the SD mechanism's employment as a basis for thermochemical kinetics submodels for multidimensional, temporally transient SFRJ combustor models. However, the number of reactions in the SD mechanism is considerably greater than the 120 limit mentioned previously (Nusca et al. 2019; Chen and McQuaid 2020). Therefore, it too will need to be reduced for that application.

Seeking to address concerns about an HR-TMM's capacity to create viable skeletal mechanisms for SFRJ combustor models, I developed and applied an HR-TMM to create skeletal versions of the SD mechanism for modeling the planned experiments (McQuaid 2020). A reasonably large number of fairly small candidates were produced, and the capacity of the smallest one to mimic the full mechanism over the ranges of pressures, oxidizer-to-fuel ratios, and solid-gas interface temperatures expected to be realized in the experiments was vetted. Comprising 63 reactions and

31 species, this mechanism will be called hereafter HR-A38.09_04.* Among other things, I confirmed that when HR-A38.09_04 was employed as the basis for simulating relevant OFDFs, key features of solutions produced with the SD mechanism were reasonably reproduced, and SD- and HR-A38.09_04-based predictions for HTPB's regression rate throughout the prescribed parameter space were in reasonable agreement with one another. Anticipating the study summarized herein, the results of that study also constitute a basis for comparing the OFDF-TMM's cost and performance to those of an HR-TMM.

This report discusses the various considerations underlying the formulation of a screening protocol for producing candidates for SFRJ-related modeling applications. Of particular importance was the selection of OFDF simulation parameter values to screen and their deviations from standards to allow. Numerous suitably sized candidates were produced, and key results of SD-mechanism-based OFDF simulations were reproduced when the smallest candidate was substituted for the SD mechanism. Regression rate predictions produced with the two mechanisms were also compared. Based on the evaluation and the results of the prior investigation, it appears that for non-premixed systems for which it is practical to set up and apply, an OFDF-TMM could be a preferable option. In addition, potential issues in developing and applying an OFDF-TMM to reduce larger mechanisms were anticipated, and means for addressing them proposed.

* In the report summarizing the effort that created and vetted HR-A38.09_04 (McQuaid 2020), I reported that it had 33 species. That count corresponded to the total number of species that were "considered"/included in the mechanism generated by the program. However, two species, namely HE and C2H6, were neither consumed nor created by any reaction in the mechanism, and neither one was included as a diluent in any of the screening protocol's HR simulations. As such, for HR-A38.09_04's incorporation into models of the system for which it was designed (and others like it), they should be eliminated, making the application-relevant count 31. HE and C2H6 were listed (and counted) because, passed down from the SD mechanism, enhanced third-body collision efficiencies were specified for them in some of the fall-off reactions, and I did not want that information "lost". Were it noted (by someone familiar with the parameterizations of those reactions), their absence would have had the potential to raise questions about the origin of the input. Moreover, if HR-A38.09_04 was to be the starting point for constructing a larger mechanism applicable to a system in which HE and/or C2H6 were relevant, it would not likely be appreciated that the information was missing and needed to be added back.

2. Detailed Finite-Rate Chemical Kinetics Mechanism Basics

A detailed finite-rate chemical kinetics mechanism is a network comprising molecular and/or atomic species (k) connected by elementary reactions (i)

$$\mathrm{aA} + \mathrm{bB} + \cdots \rightleftharpoons \mathrm{pP} + \mathrm{qQ} + \cdots, \tag{1}$$

where a, b, …, are stoichiometric coefficients for species A, B, …, respectively. It specifies parameters for calculating (molar) rates of species conversion (R_i),

$$R_i = \frac{1}{p}\frac{d[P]}{dt} = \frac{1}{q}\frac{d[Q]}{dt} = \cdots = -\frac{1}{a}\frac{d[A]}{dt} = -\frac{1}{b}\frac{d[B]}{dt} = \cdots, \tag{2}$$

via the law of mass action,

$$R_i = k_i[A]^a[B]^b \ldots - k_{-i}[P]^p[Q]^q \ldots, \tag{3}$$

where k_i and k_{-i} are forward and reverse rate coefficients, respectively (Benson 1976). For reactions for which it is assumed that interactions with "third-bodies" will not affect their rate, k_i are computed with a modified form of the Arrhenius equation,

$$k_i(T) = A_i T^{n_i} exp\left(\frac{-E_{a,i}}{R_u T}\right), \tag{4}$$

where A_i, n_i, and $E_{a,i}$ are reaction-specific constants and R_u is the universal gas constant. Values for k_{-i} are related to k_i values via the reaction's equilibrium constant. For reactions for which interactions with third bodies cannot be neglected, pressure-dependent "corrections" that modify this basic functional form are employed to account for them.

Governing equation source terms computed on the basis of this formalism include species molar conversion rates ($\dot{\omega}_k$),

$$\dot{\omega}_k = \sum_i^I \left(\upsilon_{ki}^{"} - \upsilon_{ki}^{'}\right) R_i\,, \tag{5}$$

where (for a mechanism with I reactions) $\upsilon_{ki}^{"}$ ($\upsilon_{ki}^{'}$) are the stoichiometric coefficients for i's products (reactants). The values of $\dot{\omega}_k$ coupled with species' mass-specific enthalpies (h_k) provide a basis for computing the heat-release rate (due to chemical reactions) for a constant pressure process per unit volume ($\dot{q}_{vol}$) and per unit mass ($\dot{q}_{mass}$). Those formulae are

$$\dot{q}_{vol} = -\sum_{k=1}^{K} h_k \dot{\omega}_k W_k \tag{6}$$

$$\dot{q}_{mass} = \dot{q}_{vol}/\rho_g \tag{7}$$

where for a mechanism with K species, W_k is species k's molecular weight, and ρ_g is the density of the gas. The values of $\dot{q}_{vol}$ and $\dot{q}_{mass}$ represent measures of the rate of conversion of stored chemical energy into kinetic energy.

The governing equations also include source terms to represent molecular transport/diffusion. OPPDIF computes coefficients for them based on estimates for the transport properties of pure species and a mixture averaging rule. The transport properties of pure species are based on six atomic/molecular properties. They include 1) an index indicating whether the species is monatomic, linear, or nonlinear, 2) the species' Lennard-Jones potential well depth (ε/k_b), 3) its Lennard-Jones collision diameter (σ), 4) its dipole moment (μ), 5) its polarizability (α), and 6) its rotational relaxation collision number (Z_{rot}).

3. Overview of the San Diego (SD) Mechanism

The SD mechanism was downloaded from a website maintained by the mechanism's developers (https://web.eng.ucsd.edu/mae/groups/combustion/mechanism.html). Per the website, "It was derived by beginning with simple chemical systems then proceeding gradually to more complex systems." The full mechanism for modeling C_4H_6-air combustion was assembled by combining CK 2016-12-14, CK 2002-10-01 (for JP10 chemistry), CK 2015-03-01 (for heptane chemistry), and the thermodynamic and transport property data associated with them. The (raw) assembly comprised 335 reactions and 67 species. However, some of the reactions were "exact" (as opposed to "declared") duplicates. With the exact duplicates eliminated, the mechanism had only 323 reactions.

4. Computational Methods

4.1 The Trial Mechanism Method

The foundations of the TMM (concept) are discussed elsewhere (Kotlar 2010; McQuaid 2013a). Steps performed for each reduction performed for this study included the following:

- Randomly ordering the SD mechanism's reactions.
- Sequentially eliminating (single) reactions from the ordering on a trial basis.
- For each elimination, producing solutions for OFDF problems based on the trial mechanism created by the elimination.

- Permanently eliminating the reaction if changes in the values of selected parameters of the solutions produced with the trial mechanism deviated less than specified amounts from standards produced with the full mechanism.

A species was eliminated as a consequence of all reactions involving it being eliminated.

4.2 Opposed-Flow Diffusion Flame Simulations Employed for the Screening Protocol

A slightly modified version of the (pre-commercial) CHEMKIN-III program OPPDIF (Lutz et al. 1997; Stone 2020) was employed to formulate and solve steady laminar quasi-1-D OFDF problems whose solutions were expected to resemble the planned experiments. The bounds of the parameter space expected to be probed in the experiments were provided by Dr Brian Bojko (2019). They encompassed pressures (P) that ranged from 0.3 to 6.2 atm, (mass-based) oxidizer-to-fuel ratios (O/Fs) that ranged from 5 to 40, and temperatures at the burning surface ($T^0 = T_{fuel}$) that ranged from 500 to 650 K.

Table 1 lists distinguishing parameter values of the OFDF simulations prescribed for the screening protocol. There were 18 simulations in all. Established to evaluate HR-A38.09_04's capacity to mimic the SD mechanism throughout the entire P-O/F-T_{fuel} parameter space anticipated by Dr Bojko, the set included nine different pairs of P and velocity of air at the oxidizer inlet (V_{ox}). For each P-V_{ox} pair, two problems were formulated and solved: one with T_{fuel} equal to 500 K (or in one case 525 K) and the other with it equal to 650 K.* I assumed the temperature at the oxidizer inlet (T_{ox}) would be 300 K. The velocity of the gas exiting the fuel inlet (V_{fuel}) and the distance between the fuel and oxidizer inlets ($d_{fuel\text{-}ox}$) followed from considerations discussed in the previous report (McQuaid 2020). An input deck that is representative of all those that were employed to formulate and solve the problems is provided in Appendix A.

* Although I considered it likely that T_{fuel} will be found to be a function of P and O/F, lacking specific information concerning those relationships, I treated T_{fuel} as an independent variable. Expanding the P-O/F-T_{fuel} parameter space beyond that which would be encompassed if T_{fuel} depends on P and/or O/F, from the standpoint of creating a skeletal mechanism for modeling the opposed-flow burner experiments, this approach was "conservative". That is, candidates might be larger than they needed to be, but they would be valid for the application regardless of those relationships.

Table 1 Distinguishing parameter values of the screening protocol's OFDF simulations

Sim	Press (atm)	T_{fuel} (K)	V_{fuel} (cm/s)	T_{ox} (K)	V_{ox} (cm/s)	*O/F*	$d_{fuel\text{-}ox}$ (cm)
1	0.4	525	0.345	300	2	5.4	1.25
2	0.4	500	1.500	300	17	10.1	1.25
3	0.4	500	2.380	300	54	20.3	1.25
4	1.0	500	0.268	300	2	6.6	1.25
5	1.0	500	0.840	300	17	18.1	1.25
6	1.0	500	1.400	300	54	34.6	1.25
7	6.2	500	0.085	300	1	10.6	1.25
8	6.2	500	0.111	300	2	18.5	1.25
9	6.2	500	0.298	300	17	52.5	1.25
10	0.4	650	0.350	300	2	6.5	1.25
11	0.4	650	1.640	300	17	12.0	1.25
12	0.4	650	2.620	300	54	24.0	1.25
13	1.0	650	0.277	300	2	8.3	1.25
14	1.0	650	0.920	300	17	21.7	1.25
15	1.0	650	1.550	300	54	40.5	1.25
16	6.2	650	0.090	300	1	13.0	1.25
17	6.2	650	0.118	300	2	19.9	1.25
18	6.2	650	0.318	300	17	63.3	1.25

The simulations were run and assessed sequentially in the order given. The 18 simulation-evaluations per trial mechanism is a number far greater than I have used in any prior mechanism reduction effort, including the HR-TMM-based reduction of the SD mechanism for this application (McQuaid 2020). In most previous cases, the number was limited by computational cost: the larger the number of simulations, the larger the cost. Computational cost was not an issue in the HR-TMM-based reduction of the SD mechanism. Rather, I was interested in evaluating how an HR-TMM would work for the subject application if the types of compromises that typically need to be made in formulating a screening protocol for the reduction of very large mechanisms (such as ARL's $C_{20}H_{32}$-air mechanism) were made. Since that study established that key features of solutions produced with the SD mechanism were reasonably reproduced with a relatively small candidate (viz. HR-A38.09_04), I was curious whether a protocol that attempted to ensure candidates could do so would produce similarly small candidates. In addition, hoping to reveal any issues that might arise in applying the OFDF-TMM to larger mechanisms, I wanted the screening protocol to tax the DSRC-HPC platform's computing power.

Of the 120 different orderings that were reduced (and results saved), there was a slight difference between the protocol specified for the first 60 submissions (Set A)

and that for the second 60 (Set B). As mentioned in the introduction, in order for an OFDF-TMM to be practical, OFDF problems have to be solved in a matter of seconds, and the only way that could happen was if good initial state-variable estimates were provided via restart files. The restart files employed for the first pass through Sets A and B were generated in the previous study (McQuaid 2020). For Set A, that same file set was used throughout the reduction process. Finding the OFDF-TMM feasible, but that it could afford to be sped up, I thought that might be accomplished by periodically updating the restart files, reasoning that the solutions produced with the most recently created skeletal mechanism would provide the best starting estimates for the next set of simulations. However, since there was also a computational cost associated with updating the restart files, I rewrote the program such that the restart files produced at the end of a pass were employed for the next pass through the ordering. Set B was submitted to determine if any speed-up would be realized by this approach. There was not.

4.3 Standards for Establishing the Similarity of OFDF Simulations

Comprising K+4 state-variable values at each grid point, solutions to OFDF problems can contain a considerable amount of data. For example, in the current study, the SD mechanism had $K = 67$ species, and more than 200 grid points were required to produce solutions that met the specified convergence criteria. Therefore, each solution comprised over 13,000 state-variable values. For OFDF simulations based on ARL's $C_{20}H_{32}$-air mechanism, the number is likely to be more than 10 times greater.

The premise for mechanism reduction being that not all such values are needed for a model's predictions for (global) phenomena of interest to be reliable and accurate, a critical consideration in developing a TMM implementation includes establishing which ones are needed. In addition, it is important to establish how much the values produced for them with a trial mechanism can deviate from standards established with the full mechanism and the former still be expected to produce reliable and accurate predictions for the phenomena of interest. This section discusses these aspects of the screening protocol's formulation.

In HR-TMMs that have been developed by PSB (to date), the parameters of the HR simulations that have been compared include local maxima in the $\dot{q}_{mass}$ and $\dot{q}_{vol}$ versus t histories ($\dot{q}_{mass}^{max}$ and $\dot{q}_{vol}^{max}$, respectively), the times at which those maxima occur (t_{mass}^{max} and t_{vol}^{max}, respectively), and the temperature at the end of the simulation (T_{final}). The rationale for reducing a mechanism for propulsion system modeling based on comparing these (and only these) parameters' values has been

discussed in some detail previously (McQuaid 2013b). Briefly, the comparison of $\dot{q}^{max}_{mass/vol}$ and $t^{max}_{mass/vol}$ values attempts to ensure that the skeletal mechanism will convert stored chemical energy into kinetic energy at rates (within the parameter space of interest) similar to those that would be predicted with the full mechanism, and thereby enable CFD models to well-simulate phenomena such as ignition delays and flame standoffs. The comparison of T_{final} values attempts to ensure that the skeletal mechanism can evolve the system to end states accessible via the full mechanism. More specifically, the full mechanism should be able to evolve the gas to thermodynamic equilibrium, and the skeletal mechanism needs to be able to do that as well. If it can, it increases the likelihood that the CFD model's predictions for the temperatures in the combustor will be reliable. In addition, it increases the likelihood that the model will produce a working fluid whose thermophysical properties are similar to those that would be produced with the full mechanism. That capacity is necessary for motor performance metrics such as specific impulse and thrust to be well predicted.

The "maximum allowable deviations" (MADs) between the full- and trial-mechanism-based values of these parameters that have been permitted to date are empirically based and have evolved somewhat since Dr Kotlar first introduced the HR-TMM. His program started a reduction with MADs for $\dot{q}^{max}_{mass/vol}$ and $t^{max}_{mass/vol}$ set equal to ±0.5% and the MAD for T_{final} set equal to ±10 K. Thereafter, they were increased collectively in ±0.5% and 10 K increments, respectively, and they were allowed to reach ±10% and 200 K, respectively. (Dr Kotlar did not report or tell me his rationale for this protocol. I assume it was experience based on trial and error.) To address various issues that arose when I further developed and applied HR-TMMs, I formulated and employed a different basis for computing $\dot{q}^{max}_{mass/vol}$, set initial MADs at ±1.0% and ±1.0 K, increased them collectively in ±1.0% and ±1.0 K increments, and did not allow the MAD in T_{final} to exceed ±10 K (McQuaid 2013a; Chen and McQuaid 2016). In addition, given the sensitivity of $t^{max}_{mass/vol}$ to small changes in temperature (transients), I have permitted MADs for them to reach ±21% in order to obtain candidates with targeted sizes (Chen and McQuaid 2016).

Based on the successes achieved with HR-TMMs, in the beta version of the OFDF-TMM, I formulated a screening protocol in which the values of analogs of $\dot{q}^{max}_{mass/vol}$, $t^{max}_{mass/vol}$, and T_{final} in OFDF simulations were compared. They included $\dot{q}^{max}_{mass/vol}$, the locations at which those maxima occurred ($d^{max}_{mass/vol}$), and the maximum temperature in the simulation (T_{max}). However, when (subsequently) vetting HR-TMM-produced candidates on the basis of their capacity to reproduce steady, quasi-1-D OFDF simulations produced with a full mechanism (McQuaid 2019, 2020), there was little to suggest that establishing agreement between these parameters' values (alone) would ensure candidates were capable of mimicking the

full mechanism near the burning surface, and this region is a critical determinant of regression rates. (See Section 4.4.) Moreover, it was observed that candidates could reasonably reproduce temperatures and temperature gradients near the surface as well as T_{max} and T_{max}'s location ($d_{T_{max}}$) without there being good agreement between their respective OFDF simulation's $\dot{q}^{max}_{mass/vol}$ and $d^{max}_{mass/vol}$values. As such, requiring these parameters' values to meet (arbitrary) standards could result in the skeletal candidates being larger than necessary. Therefore, for this study I revised the protocol, prescribing screening based on the temperature gradient at the second grid point [$(dT/dx)_{j=2}$, where j is the grid point's index and j = 1 corresponds to the (x = 0) burning surface], T_{max}, and $d_{T_{max}}$. Because $(dT/dx)_{j=2}$ was easily calculated (with a central difference formula) and T_{max} and $d_{T_{max}}$ were readily identifiable, the evaluation was considerably less complex to implement than the one employed for the beta version, reducing its computational cost and increasing its reliability.

As for specifying the MADs for $(dT/dx)_{j=2}$, T_{max}, and $d_{T_{max}}$ values, I wanted regression rates predicted with a skeletal mechanism to be no more than ±5% different from those predicted with the full mechanism. Therefore, given the relationship between $(dT/dx)_{j=2}$ and regression rates, the initial MAD for $(dT/dx)_{j=2}$ was set equal to ±0.5%, and it was increased in ±0.5% increments to a maximum of ±5.0%. Equating $d_{T_{max}}$ with $t^{max}_{mass/vol}$, the initial MAD for $d_{T^{max}}$ was set equal to ±1.0%, and it was increased (collectively with the MADs for $(dT/dx)_{j=2}$ and T_{max}) in ±1.0% increments up to a maximum of ±10%. Similarly, equating T_{max} with T_{final}, the initial MAD for T_{max} was set equal to ±1.0 K, and it was increased in ±1.0 K increments up to a maximum of ±10 K. Variations of this protocol that involved starting and increasing the MADs' magnitudes in larger increments were also tested to determine if runtimes could be reduced (because a fewer number of passes would be required). Although that seemed likely, the bigger question was whether such prescriptions would compromise the method's capacity to produce viably small candidates.

4.4 Regression Rate Predictions

The method employed to predict HTPB regression rates in the planned experiments is discussed in more detail in the report summarizing the prelude to this investigation (McQuaid 2020). Briefly, it is a slight a variation of the CYCLOPS framework Miller and Anderson (2000, 2004) devised to predict the burning rates of monopropellants and explosives. Derived from general equations for representing the continuities of energy, mass, and species fluxes at a planar condensed-phase–gas-phase interface, it is predicated on the assumption that chemical reactions and diffusion in the condensed phase can be neglected. When

this assumption is valid, the 1-D energy-flux-boundary condition at the interface ($x = 0$) reduces to

$$\left[\lambda_g \frac{dT}{dx}\right]^{+0} = r\rho_c\left(\sum_k^K (Y_g^k)^{-0}(h_g^k)^{+0} - h_c^{-\infty}\right) \quad (8)$$

where the left-hand side of the equation corresponds to the energy flux incident on the interface due to the thermal conductivity (λ_g) and the temperature gradient (dT/dx) adjacent to the gas-phase side of the interface ($x = +0$), and the right-hand side corresponds to the energy flux needed to raise the enthalpy of a mass flux with density ρ_c from the value for the condensed phase at $x = -\infty$ ($h_c^{-\infty}$) to that of a set of nascent gas-phase products with mass fractions Y_g^k and enthalpies h_g^k. The values of λ_g, dT/dx, and h_g^k at the interface depend on the temperature (T^0); the value of $[\lambda_g dT/dx]^{+0}$ also depends on the pressure. In the variation employed for this study, the fuel inlet corresponded the interface between the condensed and gas phases. OPDIFF supposes the fuel stream enters at $x = 0$ ($j = 1$). Therefore, T_{fuel} corresponded to T^0.

Corresponding to C_4H_6 being the only gas-phase product of HTPB's pyrolysis $[(Y_g^{C_4H_6})^{-0} = 1]$, the energy-flux-boundary condition was

$$\left[\lambda_g \frac{dT}{dx}\right]^{+0} = r\rho_c\left[(h_g^{C_4H_6})^{+0} - h_c^{-\infty}\right]. \quad (9)$$

To complete the calculation, HTPB's ρ_c and $h_c^{-\infty}$ had to be specified. As in the previous study (McQuaid 2020), ρ_c was set equal to 0.9 g/cm^3 (Shark et al. 2014) and $h_c^{-\infty}$ was set equal to –40 cal/g. The latter represented a nominal value near the middle of several from sources I was familiar with and trusted.

Also following the previous study, Eq. 9 was considered satisfied if

$$\left|\frac{r\rho_c\left[(h_g^{C_4H_6})^{+0} - h_c^{-\infty}\right]}{\left[\lambda_g \frac{dT}{dx}\right]^{+0}} - 1\right| \leq 0.01. \quad (10)$$

Its sufficiency for the purposes of the two studies derived from the observation that for a given/fixed P, V_{ox}, and T_{fuel}, the right-hand side of Eq. 9 changed monotonically and with similar magnitude (percentage-wise) as changes in V_{fuel} when the right- and left-hand sides were within a factor of 10 of one another, and the left-hand side changed (in the opposite direction) to a smaller degree. Therefore, given that mass conservation requires $r\rho_c = V_{fuel}\rho_g$ (or $r = V_{fuel}\rho_g/\rho_c$), the calculated *r's* were expected to be within 1% of the values that would be obtained if Eq. 9 was satisfied "exactly". Since in general I consider a predicted regression rate to be in good agreement with a measured rate if the two are within a factor of

2 of one another, this criterion was more than sufficient to exclude this consideration as a significant factor in any noteworthy difference.

5. Results

5.1 Candidate Generation and Selection

Of the 120 orderings for which results of the reduction process were saved, 93 of them underwent the entire prescribed protocol. (For the remainder, the entire protocol had not been completed by the end of the requested 96-h wall time, and no attempt was made to restart them.) Whether the entire protocol was completed or not, the reductions of all 120 orderings produced candidates with ≤45 species, and 118 of those candidates had ≤115 reactions. Candidates produced from 16 different orderings had ≤100 reactions and ≤40 species. Given that the parameter space encompassed by the screening protocol's simulations was likely larger than it needed to be and that the MADs for the screened parameter's values were relatively exacting, the production of candidates with sizes small enough to be employed by a CFD combustor model was encouraging.

The smallest number of species in any candidate was 37, but that candidate had 95 reactions. As such, it was considered larger (overall) than one comprising 88 reactions and 38 species. Selected for further evaluation, it will be referred to hereafter as A45.10_04, where "A45" is an initial reaction ordering designator, "10" indicates the (collective) MAD level at which it was produced, and "04" indicates the number of passes through the ordering at that level that preceded its creation. The reactions and species composing A45.10_04 are listed in Appendix B.*

5.2 Postreduction Analyses

5.2.1 Differences between Screened Parameter Values

Table 2 lists the differences between the $(dT/dx)_{j=2}$, T_{max}, and $d_{T_{max}}$ values produced with the SD mechanism and with A45.10_04 for each of the screening protocol's 18 simulations. Several observations were notable. In particular, although the MADs for $(dT/dx)_{j=2}$ and $d_{T_{max}}$ were ±5.0% and ±10%,

* As was done in listing HR-A38.09_04 (McQuaid 2020), A45.10_04's listing includes HE and C2H6, but neither one is consumed or produced by any reaction in A45.10_04, and neither one was a diluent in any of the screening protocol's simulations. Therefore, they should be eliminated from the mechanism prior to its incorporation into a CFD model. The species count given and referenced for the remainder of this report (38) reflects that expectation.

respectively, during the pass that created A45.10_04, for 17 of the 18 simulations, A45.10_04 produced $(dT/dx)_{j=2}$ values that were within 4.0% of those produced with the SD mechanism. Given the relationship between $(dT/dx)_{j=2}$ and regression rate predictions, this was a welcome result. In addition, all the A45.10_04-based values for $d_{T_{max}}$ were within 1.5% of their respective standards. As for the differences between T_{max} values produced with the SD mechanism and with A45.10_04, the discrepancies between them and the MADs for them (±10 K) were not as dramatic as in the case of $(dT/dx)_{j=2}$ and $d_{T_{max}}$, but they suggested that A45.10_04 was "comfortably" able to provide access to the end states predicted with the SD mechanism over the entire prescribed *P*-*O/F*-T_{fuel} parameter space. (That is, being randomly distributed about zero and not expanding out to the MADs allowed, the deviations observed suggest A45.10_04 will not evolve systems within this parameter space to end states that are significantly different from those that would be produced with the SD mechanism.)

Table 2 Differences (Δ) between the values of $(dT/dx)_{j=2}$, $d_{T_{max}}$, and T_{max} produced with the SD mechanism and with A45.10_04 for individual simulations

Sim	$\Delta[(dT/dx)_{j=2}]$ (%)	$\Delta d_{T_{max}}$ (%)	ΔT_{max} (K)
1	0.7	0.0	–5.8
2	–0.7	0.0	3.7
3	–1.0	–0.6	–9.1
4	–1.0	0.3	0.8
5	0.1	–0.5	8.5
6	–0.4	0.0	4.6
7	3.9	0.9	–1.8
8	3.4	1.4	–2.9
9	1.8	0.6	–8.6
10	0.6	0.0	–2.2
11	–1.0	0.0	5.6
12	–1.5	–0.6	–7.7
13	–1.8	0.2	–0.2
14	–0.1	–0.4	8.9
15	–0.7	0.0	5.9
16	4.4	0.9	–1.6
17	4.0	0.5	–2.9
18	2.0	0.6	–8.7

5.2.2 Comparisons of OFDF Simulation Results

As mentioned in the introduction, each OFDF simulation produced with the SD mechanism comprised more than 13,000 state-variable values, and the creation of A45.10_04 was based on comparing just three parameter values derived from simulations produced with trial mechanisms, namely, $(dT/dx)_{j=2}$, T_{max}, and d_T^{max}. Therefore, additional validation of A45.10_04's capacity to reproduce results produced with the SD mechanism was sought. Toward that objective, SD- and A45.10_04-based T versus d solutions from all 18 of the screening protocol's simulations were plotted in their entirety and compared to their respective standard. Given $\dot{q}_{mass}$'s role in screening and vetting candidates produced by HR-TMMs, SD- and A45.10_04-based $\dot{q}_{mass}$ versus d plots derived from the simulations were also compared.

Figs. 1–9 show the comparisons for Simulations 1–9, respectively. Again, these were all the simulations in which T_{fuel} was 500 or 525 K. The comparisons of the corresponding results obtained from T_{fuel} = 650 K simulations were qualitatively similar, and thus will not be discussed further. They are shown in Appendix C.

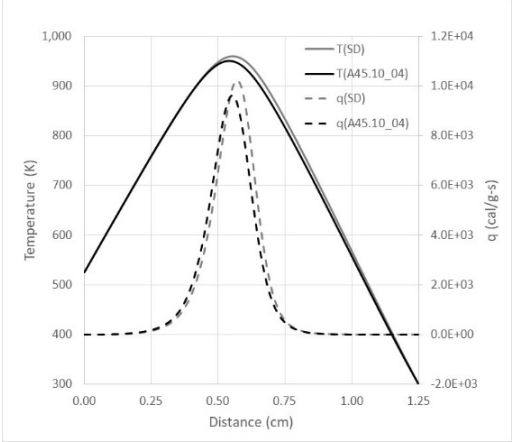

Fig. 1 Comparison of results produced with the SD mechanism and with A45.10_04 for OFDF simulation 1: P = 0.4 atm, V_{ox} = 2 cm/s, T_{fuel} = 525 K

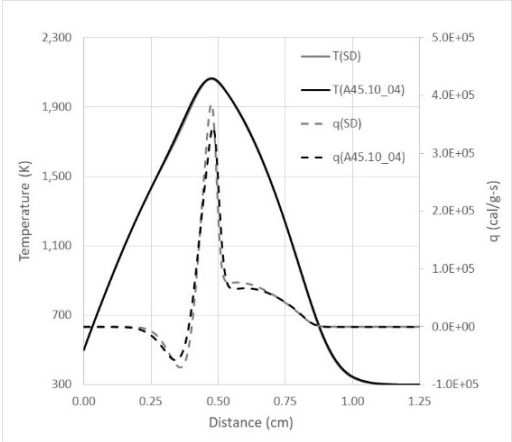

Fig. 2 Comparison of results produced with the SD mechanism and with A45.10_04 for OFDF simulation 2: P = 0.4 atm, V_{ox} = 17 cm/s, T_{fuel} = 500 K

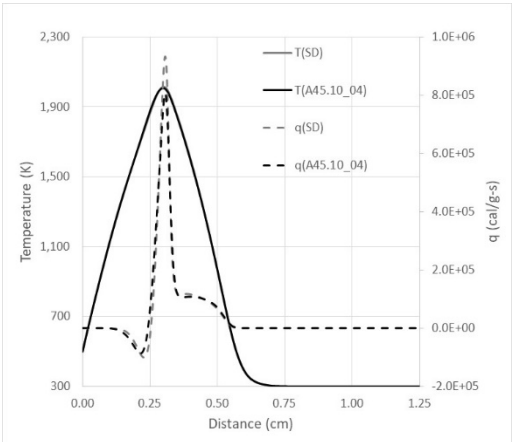

Fig. 3 Comparison of results produced with the SD mechanism and with A45.10_04 for OFDF simulation 3: P = 0.4 atm, V_{ox} = 54 cm/s, T_{fuel} = 500 K

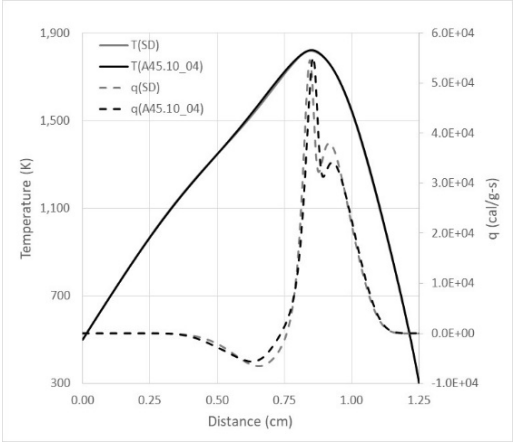

Fig. 4 Comparison of results produced with the SD mechanism and with A45.10_04 for OFDF simulation 4: P = 1.0 atm, V_{ox} = 2 cm/s, T_{fuel} = 500 K

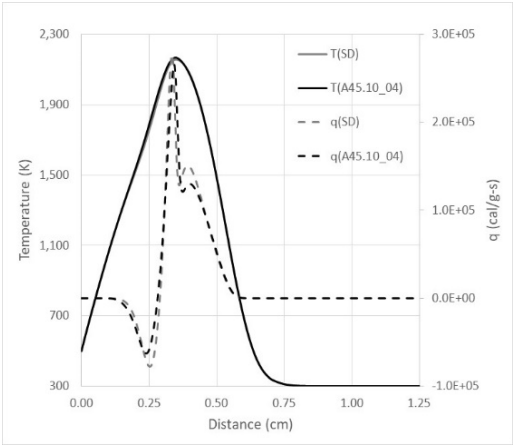

Fig. 5 Comparison of results produced with the SD mechanism and with A45.10_04 for OFDF simulation 5: P = 1.0 atm, V_{ox} = 17 cm/s, T_{fuel} = 500 K

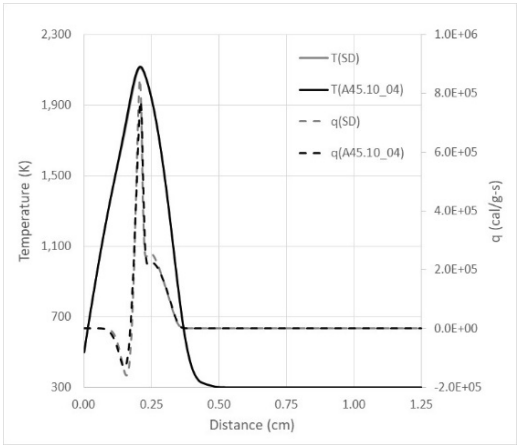

Fig. 6 Comparison of results produced with the SD mechanism and with A45.10_04 for OFDF simulation 6: P = 1.0 atm, V_{ox} = 54 cm/s, T_{fuel} = 500 K

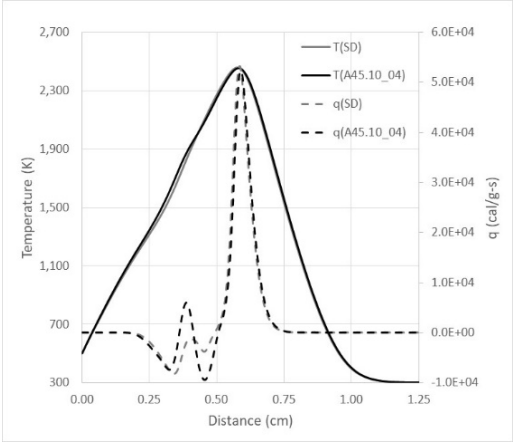

Fig. 7 Comparison of results produced with the SD mechanism and with A45.10_04 for OFDF simulation 7: P = 6.2 atm, V_{ox} = 1 cm/s, T_{fuel} = 500 K

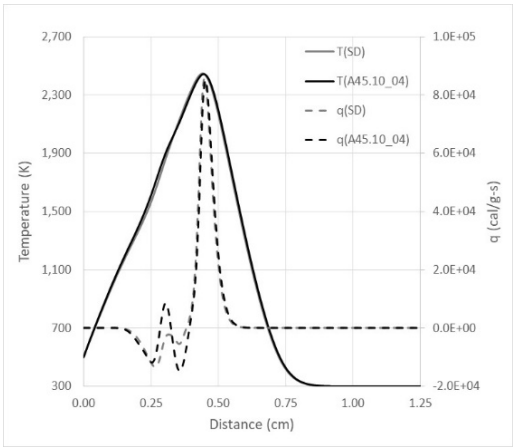

Fig. 8 Comparison of results produced with the SD mechanism and with A45.10_04 for OFDF simulation 8: P = 6.2 atm, V_{ox} = 2 cm/s, T_{fuel} = 500 K

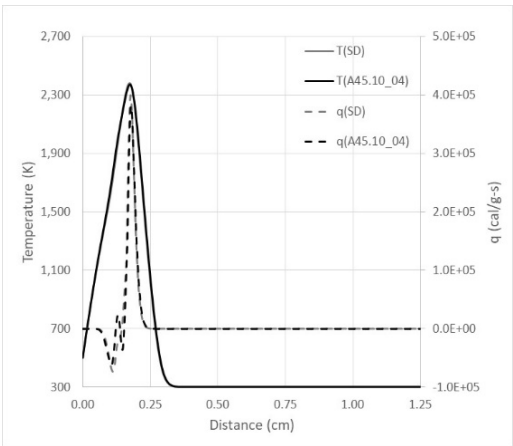

Fig. 9 Comparison of results produced with the SD mechanism and with A45.10_04 for OFDF simulation 9: P = 6.2 atm, V_{ox} = 17 cm/s, T_{fuel} = 500 K

Given that the decision to eliminate a reaction from the SD mechanism was based on screening the values of just three parameters derived from each simulation, I consider the comparisons shown in Figs. 1–9 remarkable. Although the temperature profiles are relatively featureless, except for Simulations 1 and 10, which corresponded to the lowest *P* and *O/F* of the parameter space for which A45.10_04 was designed, the $\dot{q}_{mass}$ versus d plots produced with the SD mechanism display one or two distinct exothermic transients and one or two distinct endothermic transients, and they were reasonably reproduced when A45.10_04 was employed as the basis for the simulations.

In comparison, the capacity of HR-A38.09_04 to reproduce these transients was not as good (McQuaid 2020). Quantitatively, in all cases there was much greater disagreement between the T and $\dot{q}_{mass}$ versus d plots produced on the basis of it and the SD mechanism. Moreover, in the 6.2 atm simulations, HR-A38.09_04 produced a fairly significant (spurious) exothermic transient that was not produced with the SD mechanism. While the comparison is not entirely fair,* it can still be concluded that, if an OFDF-TMM is feasible to develop and apply, it is likely to be a more cost-effective and efficient option for creating skeletal mechanisms for modeling non-premixed combustion systems. The computational and labor costs needed to set up and run the OFDF-TMM were (and will in general be) significantly higher than those for the HR-TMM. However, if the number of OFDF simulations performed and evaluated to establish an HR-TMM-generated candidate's validity is equal to the number of simulations prescribed for an OFDF-TMM's screening protocol, then the overall labor cost for producing and vetting candidates for an application will be about the same for the two variations if the first HR-TMM candidate selected for further vetting proves to be acceptable. If not, then the overall labor cost for an OFDF-TMM will be less (and possibly significantly so). Already having established that the values of three key parameters of each simulation meet standards being sought, to evaluate a candidate to the extent represented by Figs. 1–9, it is only necessary to plot results that have already been generated.

With respect to A45.10_04's ability to mimic the SD mechanism over the entire prescribed *P*-*O/F*-T_{fuel} parameter space, I was also interested in whether any species

* The objectives of the two studies were different, resulting in different considerations being bases for specifying their screening protocols. In particular, the protocol that produced HR-A38.09_04 was not nearly as comprehensive with respect to evaluating candidates at the bounds of the parameter space of interest as the one that produced A45.10_04. Therefore, not surprisingly, the smallest HR-TMM-produced candidates were smaller than A45.10_04, and HR-A38.09_04 comprised only 63 reactions and 31 species. Had the HR-TMM's screening protocol been more comprehensive or larger candidates meeting more exacting MADs been evaluated, a candidate similar in size to A45.10_04 that did not exhibit HR-A38.09_04's flaws might have been produced and found.

in the SD mechanism that was not in A45.10_04 would reach a significant concentration. Therefore, mole fraction versus distance solutions for all such species were plotted for all 18 P-V_{ox}-T_{fuel} cases. The only species that consistently reached a mole fraction that exceeded 1.0E-5 (or 0.001%) was C3H3. This was somewhat surprising to me because the same result was observed in the preceding study (McQuaid 2020), and I thought that C3H3 would be among the species included in slightly larger mechanisms. However, despite A45.10_04 having seven more species than HR-A38.09_04, C3H3 was not among them (see Table 3). As such, its absence suggests that (in both cases) reactions associated with C3H3 were eliminated from the network because the roles they played in the simulations were assumed by other parts of it.

Additionally, as in the previous study (McQuaid 2020), species in the SD mechanism that were not in A45.10_04 whose concentrations reached a mole fraction that exceeded 1.0E-5 in Simulations 1 and 10 were different than those observed in the other 16 cases. In the previous study, they included (in order of peak concentration) CH3CHO, C2H4O, C3H8, C2H5OH, and C5H10. In the current study, CH3CHO and C5H10 were in A45.10_04, and the peak concentrations of C2H4O, C3H8, and C2H5OH had magnitudes and rankings similar to those in the previous study. As such, these comparisons point to the similarity of the results produced by the two variations.

Investigating further the similarities and differences between A45.10_04 and HR-A38.09_04, I compared their species and reactions. As mentioned previously, HR-A38.09_04 had 63 reactions and 31 species, and all of the latter were in A45.10_04 (see Table 3). In addition, 55 of the 63 reactions in HR-A38.09_04 were in A45.10_04. Supplementing the results presented in the previous study, these results speak well of the HR-TMM's capacity to create skeletal mechanisms for the application. They also indicate the HR-TMM's potential to facilitate an OFDF-TMM-based reduction effort. (See Section 6.)

5.2.3 Regression Rate Predictions

Table 4 presents the HTPB regression rates predicted for each of the screening protocol's 18 P-V_{ox}-T_{fuel} cases. As discussed previously (McQuaid 2020), I was struck by two outcomes. One was that for a given P-V_{ox}, the difference between the rates produced when T_{fuel} was 500 K and when it was 650 K was not particularly significant. In general, for the same P-V_{ox} the rate predicted when T_{fuel} was 500 K was about 20% higher than when it was 650 K. I was also initially surprised by how low the predictions were. However, there is indirect evidence that suggests they will be prove to be reasonable.

Table 3 Comparison of species in A45.10_04 and HR-A38.09_04

No.	A45.10_04	HR-A38.09_04
1	N2	N2
2	AR	AR
3	H	H
4	O2	O2
5	OH	OH
6	O	O
7	H2	H2
8	H2O	H2O
9	HO2	HO2
10	H2O2	H2O2
11	CO	CO
12	CO2	CO2
13	HCO	HCO
14	CH3	CH3
15	CH4	CH4
16	CH2O	CH2O
17	T-CH2	T-CH2
18	C2H4	C2H4
19	CH3O	CH3O
20	C2H5	C2H5
21	C2H2	C2H2
22	C2H3	C2H3
23	CH2CHO	CH2CHO
24	HCCO	HCCO
25	CH2CO	CH2CO
26	CH2OH	CH2OH
27	C3H4	C3H4
28	C3H5	C3H5
29	C3H6	C3H6
30	C4H8	C4H8
31	C4H6	C4H6
32	CH3CH2O	
33	C2H4OOH	
34	CH3CHO	
35	I-C3H7	
36	CH3CO	
37	CHCHO	
38	C5H10	

Table 4 Comparison of SD- and A45.10_04-based predictions for T_{max}, $(dT/dx)_{j=2}$, and r derived from OFDF simulations for various P-V_{ox}-T_{fuel} combinations[a]

P—T_{fuel} Mechanism	V_{ox} = 1 cm/s			V_{ox} = 2 cm/s			V_{ox} = 17 cm/s			V_{ox} = 54 cm/s		
	T_{max} (K)	$\left(\frac{dT}{dx}\right)_{j=2}$ (K/cm)	r (cm/s)	T_{max} (K)	$\left(\frac{dT}{dx}\right)_{j=2}$ (K/cm)	r (cm/s)	T_{max} (K)	$\left(\frac{dT}{dx}\right)_{j=2}$ (K/cm)	r (cm/s)	T_{max} (K)	$\left(\frac{dT}{dx}\right)_{j=2}$ (K/cm)	r (cm/s)
0.4 atm—500 K		. . .			*O/F*=5.4[b]			*O/F* =10.1			*O/F* =20.3	
SD	. . .	. . .	. . .	959	9.43E+02	1.9E-04	2062	4.48E+03	8.8E-04	2004	7.09E+03	1.4E-03
A45.10_04	. . .	. . .	. . .	950	9.50E+02	1.9E-04	2065	4.45E=03	8.8E-04	2007	7.02E+03	1.4E-03
0.4 atm—650 K		. . .			*O/F* =6.5			*O/F* =12.0			*O/F* =24.0	
SD	. . .	. . .	. . .	1037	6.54E+02	1.6E-04	2062	3.09E+03	7.4E-04	2022	4.92E+03	1.2E-03
A45.10_04	. . .	. . .	. . .	1035	6.58E+02	1.6E-04	2065	3.09E+03	7.3E-04	2026	4.85E+03	1.1E-03
1.0 atm—500 K		. . .	.		*O/F* =6.6			*O/F* =18.1			*O/F* =34.6	
SD	. . .	. . .	. . .	1820	2.00E+03	3.9E-04	2158	6.26E+03	1.2E-03	2112	1.04E+04	2.0E-03
A45.10_04	. . .	. . .	. . .	1821	1.98E+03	3.9E-04	2167	6.27E+03	1.2E-03	2117	1.04E+04	2.0E-03
1.0 atm—650 K		. . .			*O/F* = 8.3			*O/F* =21.7			*O/F* =40.5	
SD	. . .	. . .	. . .	1804	1.30E+03	3.1E-04	2175	4.28E+03	1.0E-03	2131	7.20E+03	1.7E-03
A45.10_04	. . .	. . .	. . .	1803	1.28E+03	3.1E-04	2184	4.28E+03	1.0E-03	2138	7.15E+03	1.7E-03
6.2 atm—500 K		*O/F* =10.6			*O/F* =18.5			*O/F* =52.5			. . .	
SD	2457	3.90E+03	7.7E-04	2445	5.10E+03	1.0E-03	2382	1.32E+04	2.6E-03	. . .	. . .	. . .
A45.10_04	2455	4.05E+03	7.9E-04	2442	5.27E+03	1.0E-03	2373	1.34E+04	2.7E-03	. . .	. . .	. . .
6.2 atm—650 K		*O/F* =13.0			*O/F* =19.9			*O/F* =63.3			. . .	
SD	2472	2.77E+03	6.5E-04	2461	3.41E+03	8.1E-04	2401	9.08E+03	2.2E-03	. . .	. . .	. . .
A45.10_04	2470	2.72E+03	6.5E-04	2458	3.55E+03	8.5E-04	2392	9.26E+03	2.2E-03	. . .	. . .	. . .

[a] The *O/F*s shown are based on the solutions produced with the SD mechanism.
[b] T_{fuel} = 525 K

As found for the differences in the regression-rate predictions produced with the SD mechanism and with HR-A38.09_04 (McQuaid 2020), the differences between the SD- and A45.10_04–based regression-rate predictions mirrored the corresponding difference between their $(dT/dx)_{j=2}$ predictions. The largest difference was 5%, and most differences were far smaller than that. Therefore, even if the SD mechanism proves to have shortcomings as a thermochemical kinetics basis for modeling either the proposed experiments or an SFRJ's combustor dynamics, the comparisons indicated that the OFDF-TMM has the potential to create from a valid detailed mechanism a skeletal mechanism that is similarly valid.

5.3 Computational Costs and Runtime Reduction

Because computational costs could be an impediment to using an OFDF-TMM to reduce a large mechanism such as ARL's $C_{20}H_{32}$-air mechanism, the costs and runtimes observed for its application in this study warrant discussion. The 120 different orderings of the SD mechanism for which results of the reduction process were analyzed were submitted in batches of 20 to single nodes of Centennial, an SGI ICE XA at the ARL DSRC. Each node on Centennial comprised two CPU sockets, each socket had 20 cores, and two OpenMP threads were allocated to the reduction of each ordering (Stone 2020). In preliminary 1-h jobs, for reactions that ended up being permanently eliminated, the runtime of each of the screening protocol's 18 simulations generally fell in the range from 4 to 5 s, and cumulatively, the total time for the evaluation took about 80 s.

In HR-TMM-based reduction efforts, that value coupled with the nominal number of evaluations completed in 1 h would normally constitute enough information to reasonably predict the wall time needed to complete the entire prescribed protocol. Assuming the OFDF-TMM's runtimes could be similarly estimated, I requested 48 h of wall time for the first set of jobs for which I had the expectation that the entire protocol would be completed. However, that request proved to be woefully inadequate. Moreover, estimating the wall time for Set A based on how far the reduction process had progressed within 48 h, I requested 96 h for it expecting it would be sufficient for the entire process to complete, but only 39 of the 60 underwent the complete protocol within that time. This section identifies the reasons the wall times were underestimated and means for reducing runtimes based on that knowledge.

5.3.1 Terminating Solution Searches

The underpredictions of the wall times necessary for the screening protocol to complete were a consequence of the approach to solving steady-state (time-independent) 1-D OFDF problems that OPPDIF implements. A nice summary of

the approach is provided by Stone (2020). Briefly, starting with initial estimates for the state-variables' values at each grid point, it employs Newton's method to search for the solution to the steady-state equations. However, if the search is unsuccessful, the program will integrate the equations in time in an attempt to evolve the system (at least partially) toward the steady state so that a subsequent application of Newton's method has a better chance to find it. (Unfortunately, the steady state to which time integration evolves systems is often the "trivial" one. That is, all state-variable values vary monotonically between the fuel and oxidizer inlets because chemical reactions do not occur.) This sequence is repeated until a solution is found or a state is created whose time evolution takes state-variable values "out of bounds". (Values such as negative species mass fractions indicate the integration is evolving the system toward a non-physical solution, prompting the program to stop the search.) Thus, unlike HR simulations, where (in my experience) it was rare that the elimination of a reaction significantly increased their runtime, in OFDF simulations it occurred frequently, and the cost could be considerable. For example, there were reactions whose elimination increased the runtime for a single simulation to 1200 s (20 min). Prompted by the elimination of reactions that were "important" and thus significantly perturbed the system, the cost per evaluation of such reactions was incurred for every pass through the ordering because they would not be permanently eliminated. As a result, rather than fall significantly as the mechanism was reduced, the runtime per pass leveled out.

Based on these observations and my presumption that a time-integration-produced state in which a MAD for $(dT/dx)_{j=2}$, T_{max}, or d_T^{max} is exceeded will likely continue to evolve away from the standard the restart file represents, in future applications $(dT/dx)_{j=2}$, T_{max}, and d_T^{max} will be evaluated at the end of all time integrations and the search stopped if any MAD is exceeded.

In addition to time integration, another potentially expensive process is prompted when Newton's method finds a steady-state solution on a given grid, but the gradient or curvature of any of the state-variable versus distance solutions exceeds specified limits. (Alterable via the input deck and the keywords GRAD and CURV, the limits set for this study corresponded to the foundational program's defaults.) In such cases, the program will (automatically) regrid the spatial domain in ranges where either limit is exceeded, then search for a solution on the new grid. Moreover, those searches will often prompt additional time-integration sequences. As with time integration, the eliminations of important reactions are likely to prompt it and the reactions are unlikely to be permanently eliminated. Therefore, the high cost per evaluation is likely to be incurred for every pass through an ordering.

Concerned about the cost of regridding at the start of this investigation, for Set A I did not allow the total number of grid points for any solution to exceed 500. That

value, which was approximately two times the number of grid points in each restart file, was based on my doubt that any search requiring that much regridding would lead to a solution in which $(dT/dx)_{j=2}$, T_{max}, and d_T^{max} values were within specified MADs.

Concluding subsequent to Set A's processing that it was overly optimistic to expect a search requiring that much regridding to lead to an acceptable solution, for Set B I had the program conclude the evaluation (negatively) if more than 10 new points would be needed to obtain a solution meeting the specified convergence criteria. That proved helpful; the entire process completed for 54 of the 60 orderings within 96 h, and candidates were in the same size range.

That said, there was an amount of arbitrariness in the decision to conclude the evaluation based solely on the number of grid points that I was unable to reconcile. Therefore, for the next application of the method, I will have the program make the decision to forego additional regridding (and therefore end the search) based on the same criterion employed to forego additional time integration. That is, $(dT/dx)_{j=2}$, T_{max}, and d_T^{max} will be evaluated subsequent to each regrid, and if any MAD is exceeded, the search will be stopped. The rationale is the same. I presume any post-regrid state in which a MAD is exceeded will likely continue to evolve away from the standard the restart file represents.

5.3.2 Increasing MAD Magnitude Increments

In addition to runtime considerations related to solution-search procedures, I experimented (slightly) with the screening protocol to determine whether or not runtimes could be reduced by starting and increasing the MADs' magnitudes in larger increments. The hope was that similarly sized candidates could be produced without having to make as many passes through an ordering. Again, the protocol I initially devised (and will hereafter refer to as Protocol 1) was conceptually similar to Dr Kotlar's prototype, viz. multiple, small, collective step increases in MADs. While I have long been curious as to whether multiple small steps were really necessary to produce viably small candidates, the prospect that candidates might not meet size targets and therefore necessitate the submission of another costly and time-consuming set of reductions invariably dissuaded me from prescribing protocols that deviated significantly from Dr Kotlar's prototype. Thereafter, the answer was a moot point that did not seem to warrant the effort necessary to obtain it. In the current study, however, given the considerable recurring costs associated with the trial elimination of important reactions and the knowledge that they could be prohibitive, the incentive to investigate alternatives with the potential to reduce runtimes was compelling.

To evaluate the consequences of starting and increasing the MADs' magnitudes in larger increments, three variations of Protocol 1 were employed to reduce the A45 ordering. They included

- Protocol 2: ±1.0% - ±2.0% - ±2.0 K increments
- Protocol 3: ±2.5% - ±5.0% - ±5.0 K increments
- Protocol 4: ±5.0% - ±10% - ±10 K only

Up to 10 complete passes through the ordering at a given MAD level were allowed. However, in each case all the reactions that could be permanently eliminated at a given level were eliminated prior to reaching that number.

Implementing Protocol 1, the program initiated 28 passes through the ordering. The mechanism's size at the end of each pass is shown in Table 5. Since passes at a given MAD level were performed until no more reactions could be eliminated without a MAD at that level being exceeded, there were 10 passes in which no reactions were permanently eliminated. As shown in Table 5, starting and increasing the MADs at higher values indeed led to fewer passes and shorter runtimes. However, the size of the smallest candidate produced increased as well, proving there was a tradeoff.

Nevertheless, given the tremendous reduction in runtime realized via Protocol 4 and the size of the skeletal mechanism generated on that basis, I believe it could in the future prove worthwhile to perform reductions with a single-step MAD protocol prior to performing others with an envisioned multistep protocol. Results produced with it should indicate the envisioned protocol's potential to produce candidates with targeted sizes and the wall time that will be required. Moreover, if projections are poor, such runs may provide information relevant to modifying the protocol so that all objectives are met.

Table 5 Progressions of the reduction of ordering A45 produced by protocols with different MAD increment increases[a]

Level	MADs[b]	Pass	Protocol							
			1		2		3		4	
	%-%-K		Rxns	Spec	Rxns	Spec	Rxns	Spec	Rxns	Spec
1	0.5-1.0-1.0	1	172	50	. . .	. . .	. . .	. . .	. . .	. . .
		2	166	48	. . .	. . .	. . .	. . .	. . .	. . .
		3	164	48	. . .	. . .	. . .	. . .	. . .	. . .
		4	[c]	. . .	. . .	. . .	. . .	. . .	. . .	. . .
2	1.0-2.0-2.0	1	145	46	153	48	. . .	. . .	. . .	. . .
		2	135	44	144	47	. . .	. . .	. . .	. . .
		3	133	44	137	46	. . .	. . .	. . .	. . .
		4	132	44	135	45	. . .	. . .	. . .	. . .
		5	[c]	. . .	[c]	. . .	. . .	. . .	. . .	. . .
3	1.5-3.0-3.0	1	128	44	. . .	. . .	. . .	. . .	. . .	. . .
		2	127	44	. . .	. . .	. . .	. . .	. . .	. . .
		3	[c]	. . .	. . .	. . .	. . .	. . .	. . .	. . .
4	2.0-4.0-4.0	1	125	44	125	44	. . .	. . .	. . .	. . .
		2	122	44	120	43	. . .	. . .	. . .	. . .
		3	[c]	. . .	119	43	. . .	. . .	. . .	. . .
		. . .	. . .	. . .	[c]	. . .	. . .	. . .	. . .	. . .
5	2.5-5.0-5.0	1	116	43	. . .	. . .	144	56	. . .	. . .
		2	115	43	. . .	. . .	121	43	. . .	. . .
		3	[c]	. . .	. . .	. . .	[c]	. . .	. . .	. . .
6	3.0-6.0-6.0	1	[c]	. . .	116	43	. . .	. . .	. . .	. . .
		. . .	. . .	. . .	[c]	. . .	. . .	. . .	. . .	. . .
7	3.5-7.0-7.0	1	110	41	. . .	. . .	. . .	. . .	. . .	. . .
		2	[c]	. . .	. . .	. . .	. . .	. . .	. . .	. . .
8	4.0-8.0-8.0	1	[c]	. . .	107	43	. . .	. . .	. . .	. . .
		. . .	. . .	. . .	106	43	. . .	. . .	. . .	. . .
		. . .	. . .	. . .	105	43	. . .	. . .	. . .	. . .
		. . .	. . .	. . .	[c]	. . .	. . .	. . .	. . .	. . .
9	4.5-9.0-9.0	1	c	. . .	. . .	. . .	. . .	. . .	. . .	. . .
10	5.0-10-10	1	101	40	104	43	109	43	110	42
		2	95	39	c	. . .	101	42	c	. . .
		3	90	38	. . .	. . .	[c]	. . .	. . .	. . .
		4	88	38	. . .	. . .	. . .	. . .	. . .	. . .
		5	[c]	. . .	. . .	. . .	. . .	. . .	. . .	. . .
Total no. passes			28		17		6		2	
Total wall time (h)			95.5		54.25		21.5		15.2	

[a] See text for a description of the protocols' differences.

[b] The first number corresponds to the MAD for $(dT/dx)_{j=2}$. The second number corresponds to the MAD for d_{max}. The third number corresponds to the MAD for T_{max}.

[c] No reactions were eliminated by this pass.

5.3.3 Node-Level Parallelism

A set of calculations was performed to evaluate the effectiveness of the code's OpenMP-based node-level parallelism for reducing runtimes (Stone 2020). The test case for this evaluation was the reduction of the A45 ordering via Protocol 1. With two OpenMP threads allotted to the task, the runtime necessary to complete the entire protocol was 95.5 h. Repeated with 4, 8, 20, and 40 threads allocated to the task, the reductions in wall times proved to be small. Even with 40 threads allocated, the process took 87.6 h.

As discussed by Stone (2020), the computational costs of OPPDIF simulations grow exponentially with the number of grid points, and in the test cases he was given to inform his effort, most of the computational time was spent finding solutions on refined grids.* Therefore, he focused on reducing the per-iteration cost when the number of grid points was large. As a result, for any elimination that did not prompt regridding, or regridding was limited, the extra threads did not offer much benefit. Moreover, in developing OFDF-TMMs for future applications, I expect to further limit regridding. Therefore, being extremely inefficient with respect to utilizing HPC resources, parallel processing will be eschewed until a cost-effective approach can be incorporated. An obvious approach is to perform and evaluate the simulations collectively (in parallel) rather than sequentially. Unfortunately, incorporating that capability requires more effort than can currently be afforded.

5.3.4 Sequence of Simulation Evaluations

Lacking the capacity to perform and evaluate the simulations concurrently, the program performed and evaluated them sequentially. Given also that a negative evaluation (i.e., a MAD was exceeded or a solution could not be found) for any one simulation stopped a reaction from being permanently eliminated, any remaining simulations did not have to be performed, foregoing costs that would otherwise be incurred. Thus, it was advantageous to perform and evaluate the simulations in

* Because Dr Stone had been able to significantly reduce the runtimes of HR-TMM-based reductions through the introduction of node-level parallelism (Stone 2020), I thought it would be beneficial to incorporate it into the OFDF-TMM (program) and requested that he do so before I had a "real" application for which it was needed. However, to that point, I had simply demonstrated that an OFDF-TMM could reduce a small (20 reaction-9 species) mechanism for modeling H_2-O_2 combustion, and being fairly non-demanding (computationally), it was not a sufficient basis for informing his effort. To address that issue, but lacking an appreciation for how an OFDF-TMM-based reduction process would play out for a large mechanism, I gave him problems that were demanding, but the nature of those demands proved to be different in kind from those engendered by the problems prescribed for the OFDF-TMM's screening protocol.

order from those least likely to be well reproduced to those most likely to be well reproduced (to the extent that could be ascertained beforehand).

Making this point, a listing of the reasons reactions were not permanently eliminated during the pass that created A45.10_04 is provided in Appendix D. It reveals that 75 of the 88 reactions in A45.10_04 were retained because a negative evaluation was returned on the basis of results produced for Simulation 1. As discussed previously (McQuaid 2020), my attempts to obtain a nontrivial solution to an OFDF problem at the lowest values of P (0.3 atm), T_{fuel} (500 K), and O/F (5.0) of the expected parameter space were unsuccessful. Presuming that occurred because the simulation was at or near extinction conditions, I sought nontrivial solutions to problems with slightly higher P and/or T_{fuel} values and was able to obtain one for a problem with P equal to 0.4 atm and T_{fuel} equal to 525 K. However, consistent with the system being near extinction, T_{max} was only 900 K. Therefore, I suspected that, perturbed by the elimination of a reaction from the mechanism, it would be prone to evolving to the trivial solution. Such occurrences are evidenced in Appendix D. Of the 75 reactions that were retained because their elimination resulted in Simulation 1 being negatively evaluated, 23 were retained because it was going to require more than 500 grid points to produce a solution meeting the specified convergence criteria. In 17 other cases, the deviations of $(dT/dx)_{j=2}$ and d_T^{max} from their respective standards were >100% and the deviation of T_{max} was >100 K.

As a final note related to this matter, the high percentage of reactions retained because of negative evaluations returned for a simulation near extinction conditions was also observed in a study by Esposito and Chelliah (2011). They found that the number of species in a skeletal mechanism capable of reproducing a full mechanism's predictions for a system's ignition, propagation, and extinction phenomena was largely dictated by the inclusion of reactions needed to reproduce extinction phenomena.

6. Other Considerations in Reducing Larger Mechanisms

As mentioned previously, ARL's $C_{20}H_{32}$-air mechanism has been reduced for use in an SFRJ combustor model with an HR-TMM (Chen and McQuaid 2020), and that effort along with the study summarized herein anticipate some issues that will need to be resolved going forward. This section identifies those issues and proposes solutions.

6.1 Getting Started

I have on a number of occasions attempted to obtain the solution to an OFDF problem involving a mechanism the size of the SD mechanism or larger from scratch (i.e., based on very rudimentary knowledge of what the solution would look like) and have invariably been unsuccessful. Although never particularly optimistic about such attempts' chances for success, the desire for quick resolution proved irresistible. However, for systems for which the objective was to obtain burning rate *predictions*, and thus needed pure fuel exiting the fuel inlet and pure oxidizer exiting the oxidizer inlet, such attempts were destined to fail. Although I could on the basis of thermochemical equilibrium code calculations and HR simulations make some informed guesses as to what the final products and maximum temperature would be, there were many other variables requiring specification that, lacking any preexisting knowledge (such as relevant experimental observations), I did not know how to estimate. They included the separation between the fuel and oxidizer inlets ($d_{fuel\text{-}ox}$), the center of the mixing region, and the width of the mixing region. Therefore, given the need to find solutions for K+4 state variables based on very limited data, some of which may have been poorly estimated, it was foolish to try. Moreover, the failures were so complete, generating the apocalyptic message "NO SOLUTION WAS FOUND, NOT EVEN ON THE FIRST GRID", they provided no clues that could be used to work toward the solution.

Given the size of ARL's $C_{20}H_{32}$-air mechanism, I will not be tempted to solve from scratch an OFDF problem for which it is to be a basis. Rather, the 4-step procedure I employed to obtain SD-based solutions to the 18 OFDF problems composing the screening protocol employed for the current investigation will be implemented. Alluded to in the preceding report (McQuaid 2020), it targets the formulation of a symmetric OFDF problem based on an HR-TMM-produced skeletal mechanism. The conditions at the fuel and oxidizer inlets of such problems are identical and correspond to those of a PREMIX problem with an *O/F* and inlet-gas-velocity-determined fuel (mass) flux that correspond to an *O/F* and regression-rate-determined fuel flux of the system of interest. (In the previous study, it turned out my guess for the regression-rate-determined fuel flux was considerably off, but it proved not to matter.) As discussed previously (McQuaid 2020), the solutions to PREMIX problems can be anticipated to some degree by solutions to HR problems. Moreover, solutions to PREMIX problems in which the initial temperature versus distance profile estimate is relatively poor nonetheless often provide clues to improving it. Consequently, it is generally far easier to solve PREMIX problems from scratch than it is to solve OFDF problems from scratch.

Once the PREMIX problem is solved, its temperature profile is mirrored to provide an estimate for a symmetric OFDF's temperature profile, and it is the basis for specifying $d_{fuel\text{-}ox}$, the center of the mixing region (which is obvious), and the width of the mixing region. Estimates for the species' concentrations can also be obtained from the PREMIX solution. Because the solution to this OFDF problem is just the starting point for a search to obtain solutions at conditions of interest, the skeletal mechanism is a suitable basis for it. I have observed that temperature profiles produced for such problem are not spatially symmetric, raising questions about their validity. However, since the solutions to these problems are just means to an end, their validity is not particularly relevant and I have not tried to resolve the issue.

The search for solutions to OFDF problems corresponding to solid fuel-gaseous oxidizer counterflows is conducted by first solving a series of OPDF problems in which the concentration of the oxidizer in the fuel stream and/or the concentration of fuel in the oxidizer stream is incrementally decreased. For each new problem, the state-variable values of the solution to the last-solved problem are employed as initial estimates. Capable of being automated, this process/march is continued until the fuel stream is pure fuel and the oxidizer stream is pure oxidizer.

Lastly, with the species and reactions of a larger skeletal mechanism that was generated and saved during the course of the process that produced the skeletal mechanism employed for the march added back, the problem is solved again. The restart file produced by a mechanism with fewer species, of course, has to include estimates for the mass fractions of newly added species. Relying on OPPDIF's ability to find solutions, I simply specify the initial mass fractions for newly added species to be zero throughout the entire spatial domain. This procedure is repeated until the full mechanism (or some suitably large portion of it) is restored.

From there, several options are available for obtaining solutions at other conditions of interest. One is to incrementally march full-mechanism-based solutions to the conditions of interest. Another is to incrementally march skeletal-mechanism-based solutions to the conditions of interest, then add back species and reactions. Because such marches can be automated and failures to find converged solutions for intermediate steps have to be "manually" resolved and the march restarted, I have favored marching skeletal-mechanism-based solutions because they proceeded faster and appeared to be less prone to failure, and thus (presumably) incurred less labor cost.

6.2 Screening Protocol Parameter Space Coverage and MADs

In the HR-TMM-based effort to reduce ARL's $C_{20}H_{32}$-air mechanism for modeling HTPB-air combustion in a connected-pipe SFRJ combustor (Chen and McQuaid. 2020), the screening protocol prescribed six simulations and "standard" MADs intended to ensure candidates would mimic the full mechanism over the entire prescribed *P*-*O/F*-T_{fuel} parameter space, but no candidate with <166 reactions and <128 species was produced. Subsequently suspecting that two simulations prescribed to ensure candidates would mimic the full mechanism at the low end of the expected *P*-T_{fuel} range might not be relevant, they were eliminated from the screening protocol and another set of reductions initiated. A candidate with 128 reactions and 106 species was produced, and when it was substituted for the full mechanism as a basis for the two simulations that were eliminated, results of the full-mechanism-based simulations were reasonably reproduced. The primary differences were in the simulations' t_{mass}^{max} values. Such values can be sensitive to small changes in temperature, and that proved to be the case in these two simulations. Specifically, the simulations' t_{mass}^{max} values could be brought into agreement with one another by changing the initial temperature of one of them less than 2%. Therefore, there was reason to expect that this candidate would reasonably mimic the full mechanism down to the originally prescribed parameter space's low *P*-T_{fuel} boundary.

Similarly, in the HR-TMM-based effort to reduce the SD mechanism for modeling the planned opposed-flow burner experiments (McQuaid 2020), no simulation was (intentionally) included to ensure that candidates would mimic the full mechanism at the low or high ends of the expected pressure range. In addition, the initial temperature of each of the screening protocol's three HR simulations was above the expected surface temperature range's high end. Nevertheless, when the smallest candidate produced with the protocol—namely, HR-A38.09_04—was substituted for the full mechanism as a basis for the 18 OFDF simulations discussed herein, key features of the full-mechanism-based simulations were reasonably reproduced in all cases.

Because similar compromises will likely be necessary to reduce the $C_{20}H_{32}$-air mechanism for modeling the planned experiments and future SFRJ-related applications, the reasons that reactions were retained in A45.10_04 are worth noting. Again, 75 reactions were retained because of Simulation 1 and that is more than the total number of reactions in HR-A38.09_04. Being at an extreme of the *P*-*O/F*-T_{fuel} parameter space, Simulation 1 was to this application what "off-design" conditions are to an SFRJ combustor model. As such, if one is unable to include and/or equally weight simulations intended to ensure skeletal candidates can mimic

the full mechanism over the entire relevant parameter space because the size required to do so is too large, the natural inclination would be to eliminate the equivalent of Simulation 1. It would represent a small fraction (time-wise) of the conditions in an SFRJ combustor during its flight, and the computational cost incurred because of it would not be commensurate with this measure of importance. However, to my knowledge, phenomena at off-design conditions such as ignition, propagation, and extinction are more difficult to predict than phenomena at on-design conditions, and it is precisely for this reason that the cost to develop and employ a detailed mechanism is borne. Thus, one's objectives need to be well defined when prescribing a screening protocol, and its elements weighted (by tailoring MAD specifications) accordingly.

As for the MADs that were prescribed in this investigation, as already mentioned, the differences between the SD- and A45.10_04-based $(dT/dx)_{j=2}$, and d_T^{max} values did not expand, respectively, to the ±5% and ±10% values that were allowed. Moreover, for the vast majority of cases in which a (nontrivial) trial-mechanism-based solution was found but negatively evaluated, the only reason was that the MAD for T_{max} (±10 K) was exceeded. As such, these results suggest reaction eliminations that perturbed $(dT/dx)_{j=2}$ and d_T^{max} beyond the prescribed MADs produced "big" (non-recoverable) failures, and therefore mechanism sizes cannot be reduced significantly by increasing the MADs for them.

As for increasing the MAD for T_{max}, it is worth noting that Dr Kotlar allowed deviations in T_{final} up to ±200 K for an HR simulation in which the difference between the initial and final temperature was approximately 3000 K (Kotlar 2010). For all the HR-TMM-based reductions I have performed, I limited deviations in T_{final} to ≤ ±10 K because I found that the tighter acceptance criterion significantly reduced the number of "false positives" that the method produced. (False positives are candidates that satisfy all the screening criteria but are found to have significant shortcomings when T and $\dot{q}_{mass}$ versus t histories produced with them are plotted in their entirety.) Again, the MADs to allow depend on one's objectives. In this study the adiabatic flame temperature was more than 350 K higher than the temperature of the burning surface in every simulation. Therefore, I suspect that a ±20–25 K MAD for T_{max} would have been sufficient to ensure that skeletal candidates would produce end states similar to those produced with the full mechanism, and smaller candidates thereby produced. By extension, MADs for T_{max} > ±10 K might be worth considering for future applications if candidates are exceeding targeted sizes.

7. Summary and Conclusions

To evaluate the feasibility and potential of an OFDF-TMM to produce skeletal mechanisms that are valid and practical bases for simulating reacting flows in SFRJ combustors, an implementation was developed and applied to create from the 323 reaction-67 species SD mechanism candidates for simulating the combustion of HTPB-air in an opposed-flow burner. The effort included formulating and testing a screening protocol for determining whether or not reactions were needed for the skeletal mechanism to mimic the SD mechanism in models designed to simulate the experiments. Suggested by prior studies, it prescribed comparing full- and trial-mechanism-based values for just three parameters obtained from each OFDF simulation: $(dT/dx)_{j=2}$, T_{max}, and d_T^{max}. Screening based on $(dT/dx)_{j=2}$ was prescribed in recognition of the relationship between solid-fuel regression rates and the temperature gradient in the gas adjacent to the fuel's regressing surface. Hoping to achieve skeletal-mechanism-based regression rate predictions that were within 5% of those predicted with the full mechanism, deviations in $(dT/dx)_{j=2}$ up to that magnitude were allowed. The magnitudes of the allowable deviations in T_{max} and d_T^{max} were specified based on past experience in setting standards for the values of analogous parameters that have been compared in HR-TMM screening protocols.

To produce skeletal mechanisms for modeling the planned opposed-flow burner experiments, solutions to 18 different OFDF problems were analyzed to assess a trial mechanism's potential to mimic the full mechanism over the entire parameter space expected to be realized in them. Despite this number, which is far greater than has been used in any prior HR-TMM-based reduction effort (at ARL), the OFDF-TMM was able to produce within a reasonable wall time from 120 different reaction orderings 16 candidates with ≤100 reactions and ≤40 species. The smallest, which was named A45.10_04, comprised 88 reactions and 38 species, and its capacity to reproduce simulations produced with the SD mechanism was further evaluated. Although generated on the basis of a screening protocol that only evaluated a trial mechanism's ability to reasonably reproduce $(dT/dx)_{j=2}$, T_{max}, and d_T^{max} values, remarkably good agreement between the T and $\dot{q}_{mass}$ versus d profiles produced with A45.10_04 and with the SD mechanism was observed in all 18 cases. In addition, the regression rate predictions produced with the two mechanisms were within 5% of one another for each of the 18 cases, further affirming the method's potential to produce candidates that are valid for combustor modeling applications.

Beyond the OFDF-TMM's feasibility and merit for the application, its cost and performance were compared to those of an HR-TMM developed and employed

previously for the same purpose. Due to differences in the comprehensiveness of the screening protocols employed for the two studies, the comparisons of performance—viz. candidate size versus capacity to mimic the full mechanism over the entire prescribed parameter space—did not conclusively demonstrate the OFDF-TMM's superiority for non-premixed combustion applications. For the specific application considered herein, the two approaches were competitive.

A disadvantage of the OFDF-TMM is that it is far more difficult and costly to set up and run than an HR-TMM. (Indeed, for large mechanisms, an HR-TMM-based reduction will likely be needed to set up an OFDF-TMM.) However, if the cost of validating candidates is included, the overall costs for the two methods become comparable if the first HR-TMM-generated candidate selected for additional vetting proves viable. Otherwise, the OFDF-TMM's cost will be less. Moreover, to the extent that OFDF simulations can be expected to be a better basis upon which to establish the importance of reactions and species for non-premixed systems, an OFDF-TMM should have more potential to produce smaller candidates for such applications. For modeling off-design conditions in an SFRJ combustor, this added potential may be indispensable in obtaining sufficiently small candidates from full mechanisms that are considerably larger than the SD mechanism. Issues in developing and applying an OFDF-TMM to reduce larger mechanisms were anticipated, and means for addressing them proposed.

8. References

Benson SW. Thermochemical kinetics. New York (NY): John Wiley and Sons; 1976.

Bojko B. Naval Air Warfare Center, China Lake, CA. Personal communication, 2019 July 24.

Chen CC, McQuaid MJ. Thermochemical and kinetic studies of the pyrolysis of hydroxyl-terminated polybutadiene (HTPB). Presented at the 43rd JANNAF Combustion Subcommittee Meeting; 2009 Dec 7–11; La Jolla, CA.

Chen CC, McQuaid MJ. Thermochemistry and kinetics modeling of hydroxyl-terminated polybutadiene-red fuming nitric acid (HTPB-RFNA) systems. Presented at the 5th JANNAF Liquid Propulsion Subcommittee Meeting; 2010 May 3–7; Colorado Springs, CO.

Chen CC, McQuaid MJ. Thermochemistry and kinetics modeling of the oxidation of hydroxyl-terminated polybutadiene in air. Presented at the 44th JANNAF Combustion Subcommittee Meeting, 2011 Apr 18–22; Arlington, VA.

Chen CC, McQuaid MJ. Thermochemical and kinetics modeling pertaining to AP-HTPB composite propellant combustion. Presented at the 39th JANNAF Propellant and Explosives Development and Characterization Meeting; 2015 Dec 7–10, Salt Lake City, UT.

Chen CC, McQuaid MJ. A skeletal, gas-phase, finite-rate, chemical kinetics mechanism for modeling the deflagration of ammonium perchlorate-hydroxyl-terminated polybutadiene composite propellants. Aberdeen Proving Ground (MD): Army Research Laboratory (US): 2016 Apr. Report No.: ARL-TR-7655.

Chen CC, McQuaid MJ. A skeletal finite-rate chemical kinetics mechanism for modeling HTPB-air combustion in a gun-launched solid-fuel ramjet combustor. Aberdeen Proving Ground (MD): CCDC Army Research Laboratory; 2020 Jan. Report No.: ARL-TR-8891.

Esposito G, Chelliah HK. Skeletal reaction models based on principle component analysis: application to ethylene-air ignition, propagation and extinction phenomena. Combustion and Flame 2011;158;477-489.

Kee RJ, Grcar JF, Smooke MD, Miller JA. PREMIX: a Fortran program for modeling steady laminar one-dimensional premixed flames. Livermore (CA): Sandia National Laboratories (US); 1985 Mar. Report No.: SAND85-8240.

Kotlar AJ. A general approach for the reduction of chemical reaction mechanisms. I: methodology and application to MMH-RFNA. Presented at the 5th JANNAF Liquid Propulsion Subcommittee Meeting; 2010 May 3–7; Colorado Springs, CO.

Krishnan S, George P. Solid fuel ramjet combustor design. Progress in Aerospace Sciences. 1998;34:219–256.

Lutz, AE, Kee RJ, Grcar JF, Rupley FM. OPPDIF: a Fortran program for computing opposed-flow diffusion flames. Albuquerque (NM): Sandia National Laboratories; 1997. Report No.: SAND96-8243.

McQuaid MJ. The trial mechanism method for chemical kinetics mechanism reduction: an approach to developing mechanisms with wider ranges of applicability. Presented at the 7th JANNAF Liquid Propulsion Subcommittee Meeting; 2013a Apr 29–May 2; Colorado Springs, CO.

McQuaid MJ. Chemical kinetics mechanism reduction based on principal component analysis: development and testing of some new implementations. Aberdeen Proving Ground (MD): Army Research Laboratory (US); 2013b May. Report No.: ARL-TR-6449.

McQuaid MJ. Modeling the combustion of opposed flows of butadiene and air: a skeletal finite rate chemical kinetics mechanism derived from the San Diego mechanism and regression rate predictions for hydroxyl-terminated polybutadiene-air systems. Aberdeen Proving Ground (MD): CCDC Army Research Laboratory; 2020 Mar. Report No.: ARL-TR-8918.

McQuaid MJ, Chen CC, Veals JD. Modeling ammonia borane-red fuming nitric acid combustion. Part 2: detailed finite-rate chemical kinetics mechanism reduction and validation. Presented at the 49th JANNAF Combustion Subcommittee Meeting; 2019 June 3–7; Dayton, OH.

Miller MS, Anderson WR. Energetic-material combustion modeling with elementary gas-phase reactions: a practical approach. In: Yang V, Brill TB, Ren WZ, editors. Solid propellant combustion chemistry, combustion, and motor interior ballistics. Progress in Astronautics and Aeronautics. Reston (VA): AIAA; 2000;185:501–531.

Miller MS, Anderson WR. Burning rate predictor for multi-ingredient propellants: nitrate ester propellants. Journal of Propulsion and Power 2004;20:440–454.

Nusca MJ, Minnicino M, Chen CC, Isert S, McBain A. Multidisciplinary gun-launched solid fuel ramjet (SFRJ) projectile study – initial CFD modeling results. Presented at the 49th JANNAF Combustion Subcommittee Meeting; 2019 3–7 June; Dayton, OH.

Shark SC, Zaseck CR, Pourpoint TL, Son SF. Solid-fuel regression rates and flame characteristics in an opposed-flow burner. Journal of Propulsion and Power 2014; 30:1675-1682.

Stone CP. Summary of user productivity enhancement, technology transfer, and training (PETTT) refactoring assistance for chemical kinetics analysis tools at CCDC Army Research Laboratory. Aberdeen Proving Ground (MD): CCDC Army Research Laboratory; 2020 Jan. Report No.: ARL-CR-0843.

Appendix A. A Representative Input Deck for Opposed-Flow Diffusion Flame Simulations

The program employed to formulate and solve the opposed-flow diffusion flame problems discussed in this report was a slightly modified version of the (pre-commercial) CHEMKIN-III program OPPDIF.[1,2] Problems were formulated via an input "deck". Table A-1 is representative of all that were submitted. Each line began with a keyword that prompted the program to specify the value of some parameter (or parameters). For their definitions, see the OPPDIF manual.[1] Searches for solutions to new problems were facilitated by specifying (good) initial estimates for state variables provided via a restart file. Only the parameter values specified via PRES-, VFUE-, VOXI-, and TFUE-led lines were varied. For any parameter value not specified via the input deck, the default set by the foundational program was used.[1]

Table A-1 Representative input deck for opposed-flow diffusion flame simulations

```
RSTR
MIX
ENRG
PRES 0.4
VFUE 0.3450E+00
VOXI 2.0000E+00
TFUE 525.
TOXI 300.
XEND 1.250
IRET 20
UFAC 2.
SFLR -1.E-4
PRNT 2
TIME 200 1.E-6
TIM2 200 1.E-6
GRAD 0.1
CURV 0.5
FUEL C4H6 1.00
OXID N2   0.78
OXID O2   0.21
OXID AR   0.01
KOUT C4H6 N2 O2 H2O CO CO2
RTOL 1.E-3
ATOL 1.E-6
ATIM 1.E-6
RTIM 1.E-3
END
```

[1] Lutz, AE, Kee RJ, Grcar JF, Rupley FM. OPPDIF: a Fortran program for computing opposed-flow diffusion flames. Albuquerque (NM): Sandia National Laboratories; 1997. Report No.: SAND96-8243.

[2] Stone CP. Summary of user productivity enhancement, technology transfer, and training (PETTT) refactoring assistance for chemical kinetics analysis tools at CCDC Army Research Laboratory. Aberdeen Proving Ground (MD), Army Research Laboratory (US), 2020 Jan. Report No.: ARL-CR-0843.

Appendix B. A45.10_04's Species, Reactions, and Reaction Rate-Coefficient Parameterizations

Table B-1 lists the species, elementary reactions, and parameterizations of the reactions' rate-coefficient formulae that composed A45.10_04. The table was produced by a pre-commercial CHEMKIN III "pre-processor"/mechanism interpreter. All the data in the input files came from the San Diego mechanism. They were downloaded from https://web.eng.ucsd.edu/mae/groups/combustion/mechanism.html.

As noted in the main body of the report, A45.10_04 "considers" 40 species. Among them are N2 and AR, which are not produced or consumed by any reaction. However, as constituents of the oxidizer stream in the opposed-flow diffusion flame (OFDF) simulations employed for the screening protocol, they influenced the results indirectly as third-body colliders and they will play that role in the application for which A45.10_04 was designed. Therefore, they need to be retained. Conversely, it also includes HE and C2H6, neither of which are produced or consumed by any reaction in A45.10_04, and neither was included as a diluent in any of the simulations that composed the screening protocol that produced it. They are included in the listing because enhanced third-body collision efficiencies were specified for them in some of the fall-off reactions in the San Diego (SD) mechanism, and I did not want that information separated from them in this report. Were it noted (by someone familiar with the parameterizations of those reactions), I thought it might raise questions about the origin of the input. Moreover, if A45.10_04 was to be the starting point for building a larger mechanism for a system in which HE and/or C2H6 were relevant, it would not likely be appreciated that the information was missing and needed to be added back. That said, if A45.10_04 is to be used in a reacting flow model, HE and C2H6 should be eliminated from it.

Table B-1 Species, elementary reactions, and rate-coefficient parameters that composed A45.10_04

```
 CHEMKIN-III GAS-PHASE MECHANISM INTERPRETER:
 DOUBLE PRECISION Vers. 6.3 97/01/25
 Copyright 1995, Sandia Corporation.
 The U.S. Government retains a limited license in this software.


                    --------------------
                    ELEMENTS     ATOMIC
                    CONSIDERED   WEIGHT
                    --------------------
                     1. N       14.0067
                     2. AR      39.9480
                     3. HE      4.00260
                     4. H       1.00797
                     5. O       15.9994
                     6. C       12.0112
                    --------------------
```

SPECIES CONSIDERED	PHASE	CHARGE	MOLECULAR WEIGHT	TEMPERATURE LOW	TEMPERATURE HIGH	ELEMENT COUNT N	AR	HE	H	O	C
1. N2	G	0	28.01340	300	5000	2	0	0	0	0	0
2. AR	G	0	39.94800	300	5000	0	1	0	0	0	0
3. HE	G	0	4.00260	300	5000	0	0	1	0	0	0
4. H	G	0	1.00797	300	5000	0	0	0	1	0	0
5. O2	G	0	31.99880	300	5000	0	0	0	0	2	0
6. OH	G	0	17.00737	300	5000	0	0	0	1	1	0
7. O	G	0	15.99940	300	5000	0	0	0	0	1	0
8. H2	G	0	2.01594	300	5000	0	0	0	2	0	0
9. H2O	G	0	18.01534	300	5000	0	0	0	2	1	0
10. HO2	G	0	33.00677	300	5000	0	0	0	1	2	0
11. H2O2	G	0	34.01474	300	5000	0	0	0	2	2	0
12. CO	G	0	28.01055	300	5000	0	0	0	0	1	1
13. CO2	G	0	44.00995	300	5000	0	0	0	0	2	1
14. HCO	G	0	29.01852	300	5000	0	0	0	1	1	1
15. CH3	G	0	15.03506	300	5000	0	0	0	3	0	1
16. CH4	G	0	16.04303	300	5000	0	0	0	4	0	1
17. CH2O	G	0	30.02649	300	5000	0	0	0	2	1	1
18. T-CH2	G	0	14.02709	300	5000	0	0	0	2	0	1
19. C2H4	G	0	28.05418	300	5000	0	0	0	4	0	2
20. CH3O	G	0	31.03446	300	5000	0	0	0	3	1	1
21. C2H5	G	0	29.06215	300	5000	0	0	0	5	0	2
22. C2H6	G	0	30.07012	300	5000	0	0	0	6	0	2
23. C2H2	G	0	26.03824	300	5000	0	0	0	2	0	2
24. C2H3	G	0	27.04621	300	5000	0	0	0	3	0	2
25. CH2CHO	G	0	43.04561	300	5000	0	0	0	3	1	2
26. HCCO	G	0	41.02967	300	5000	0	0	0	1	1	2
27. CH2CO	G	0	42.03764	300	5000	0	0	0	2	1	2
28. CH2OH	G	0	31.03446	300	5000	0	0	0	3	1	1
29. C3H4	G	0	40.06533	300	5000	0	0	0	4	0	3
30. C3H5	G	0	41.07330	300	5000	0	0	0	5	0	3
31. C3H6	G	0	42.08127	300	5000	0	0	0	6	0	3
32. C4H8	G	0	56.10836	300	5000	0	0	0	8	0	4
33. C4H6	G	0	54.09242	300	3000	0	0	0	6	0	4
34. CH3CH2O	G	0	45.06155	300	5000	0	0	0	5	1	2
35. C2H4OOH	G	0	61.06095	300	5000	0	0	0	5	2	2
36. CH3CHO	G	0	44.05358	300	5000	0	0	0	4	1	2
37. I-C3H7	G	0	43.08924	300	5000	0	0	0	7	0	3
38. CH3CO	G	0	43.04561	300	5000	0	0	0	3	1	2
39. CHCHO	G	0	42.03764	200	3000	0	0	0	2	1	2
40. C5H10	G	0	70.13545	300	5000	0	0	0	10	0	5

	REACTIONS CONSIDERED			(k = A T**b exp(-E/RT)) A	b	E
1.	H+O2<=>OH+O			3.52E+16	-0.7	17069.8
2.	H2+OH<=>H2O+H			1.17E+09	1.3	3635.3
3.	H2O+O<=>2OH			7.00E+05	2.3	14548.3
4.	H+OH+M<=>H2O+M			4.00E+22	-2.0	0.0
	AR	Enhanced by	3.800E-01			
	HE	Enhanced by	3.800E-01			
	H2	Enhanced by	2.500E+00			
	H2O	Enhanced by	1.200E+01			
	CO	Enhanced by	1.900E+00			
	CO2	Enhanced by	3.800E+00			
5.	H+O2(+M)<=>HO2(+M)			4.65E+12	0.4	0.0
	AR	Enhanced by	7.000E-01			
	HE	Enhanced by	7.000E-01			
	H2	Enhanced by	2.500E+00			
	H2O	Enhanced by	1.600E+01			
	CO	Enhanced by	1.200E+00			
	CO2	Enhanced by	2.400E+00			
	C2H6	Enhanced by	1.500E+00			
	Low pressure limit:	0.57500E+20	-0.14000E+01	0.00000E+00		
	TROE centering:	0.50000E+00	0.10000E-29	0.10000E+31		
6.	HO2+H<=>2OH			7.08E+13	0.0	294.9
7.	HO2+H<=>H2+O2			1.66E+13	0.0	822.9
8.	HO2+O<=>OH+O2			2.00E+13	0.0	0.0
9.	HO2+OH<=>H2O+O2			7.00E+12	0.0	-1094.7
	Declared duplicate reaction...					
10.	2OH(+M)<=>H2O2(+M)			9.55E+13	-0.3	0.0
	AR	Enhanced by	7.000E-01			
	HE	Enhanced by	4.000E-01			
	H2	Enhanced by	2.500E+00			
	H2O	Enhanced by	6.000E+00			
	H2O2	Enhanced by	6.000E+00			
	CO	Enhanced by	1.500E+00			
	CO2	Enhanced by	2.000E+00			
	Low pressure limit:	0.27600E+26	-0.32000E+01	0.00000E+00		
	TROE centering:	0.57000E+00	0.10000E+31	0.10000E-29		
11.	2HO2<=>H2O2+O2			1.03E+14	0.0	11042.1
	Declared duplicate reaction...					
12.	2HO2<=>H2O2+O2			1.94E+11	0.0	-1408.9
	Declared duplicate reaction...					
13.	H2O2+H<=>HO2+H2			2.30E+13	0.0	7950.1
14.	H2O2+H<=>H2O+OH			1.00E+13	0.0	3585.1
15.	H2O2+OH<=>H2O+HO2			1.74E+12	0.0	1434.0
	Declared duplicate reaction...					
16.	H2O2+OH<=>H2O+HO2			7.59E+13	0.0	7272.9
	Declared duplicate reaction...					
17.	CO+OH<=>CO2+H			4.40E+06	1.5	-740.9
18.	CO+HO2<=>CO2+OH			2.00E+13	0.0	22944.5
19.	HCO+M<=>CO+H+M			1.86E+17	-1.0	17000.5
	H2	Enhanced by	1.900E+00			
	H2O	Enhanced by	1.200E+01			
	CO	Enhanced by	2.500E+00			
	CO2	Enhanced by	2.500E+00			
20.	HCO+O2<=>CO+HO2			7.58E+12	0.0	409.9
21.	HCO+CH3<=>CO+CH4			5.00E+13	0.0	0.0
22.	CH2O+H<=>HCO+H2			5.74E+07	1.9	2748.6
23.	CH2O+O<=>HCO+OH			3.50E+13	0.0	3513.4
24.	CH2O+OH<=>HCO+H2O			3.90E+10	0.9	406.3
25.	CH2O+HO2<=>HCO+H2O2			4.11E+04	2.5	10210.3
26.	CH4+OH<=>H2O+CH3			1.60E+07	1.8	2782.0

```
27. CH3+H<=>T-CH2+H2                                  1.80E+14    0.0    15105.2
28. CH3+O<=>CH2O+H                                    8.43E+13    0.0        0.0
29. CH3+T-CH2<=>C2H4+H                                4.22E+13    0.0        0.0
30. CH3+HO2<=>CH3O+OH                                 5.00E+12    0.0        0.0
31. H+CH3(+M)<=>CH4(+M)                               1.35E+14    0.1       87.7
    AR              Enhanced by    7.000E-01
    H2              Enhanced by    2.000E+00
    H2O             Enhanced by    1.600E+01
    CO              Enhanced by    1.500E+00
    CO2             Enhanced by    2.000E+00
    CH4             Enhanced by    4.000E+00
    Low pressure limit:  0.15900E+34 -0.47610E+01  0.24323E+04
    TROE centering:      0.83400E+00  0.36800E+02  0.77800E+03  0.24643E+04
32. T-CH2+O2<=>CO2+H2                                 2.63E+12    0.0     1491.4
33. T-CH2+O2<=>CO+OH+H                                6.58E+12    0.0     1491.4
34. C2H2+HO2<=>CHCHO+OH                               1.60E+08    1.4    15420.0
35. CHCHO+O2=CH2O+CO+O                                1.30E+06    2.4     1604.0
36. CH3O+M<=>CH2O+H+M                                 7.78E+13    0.0    13513.4
    AR              Enhanced by    7.000E-01
    H2              Enhanced by    2.000E+00
    H2O             Enhanced by    6.000E+00
    CO              Enhanced by    1.500E+00
    CO2             Enhanced by    2.000E+00
    CH4             Enhanced by    2.000E+00
37. C2H5+O2<=>C2H4OOH                                 2.00E+12    0.0        0.0
38. C2H4OOH<=>C2H4+HO2                                4.00E+34   -7.2    23000.0
39. C2H5(+M)<=>C2H4+H(+M)                             1.11E+10    1.0    36768.6
    AR              Enhanced by    7.000E-01
    H2              Enhanced by    2.000E+00
    H2O             Enhanced by    6.000E+00
    CO              Enhanced by    1.500E+00
    CO2             Enhanced by    2.000E+00
    CH4             Enhanced by    2.000E+00
    Low pressure limit:  0.39900E+34 -0.49900E+01  0.40000E+05
    TROE centering:      0.16800E+00  0.12000E+04  0.10000E-29
40. C2H4+H<=>C2H3+H2                                  4.49E+07    2.1    13360.4
41. C2H4+OH<=>C2H3+H2O                                5.53E+05    2.3     2963.7
42. C2H4+O<=>CH3+HCO                                  2.25E+06    2.1        0.0
43. 2C2H4<=>C2H3+C2H5                                 5.01E+14    0.0    64700.1
44. C2H4+O2<=>C2H3+HO2                                4.22E+13    0.0    57623.1
45. C2H3+H<=>C2H2+H2                                  4.00E+13    0.0        0.0
46. C2H3(+M)<=>C2H2+H(+M)                             6.38E+09    1.0    37626.7
    AR              Enhanced by    7.000E-01
    H2              Enhanced by    2.000E+00
    H2O             Enhanced by    6.000E+00
    CO              Enhanced by    1.500E+00
    CO2             Enhanced by    2.000E+00
    CH4             Enhanced by    2.000E+00
    Low pressure limit:  0.15100E+15  0.10000E+00  0.32686E+05
    TROE centering:      0.30000E+00  0.10000E+31  0.10000E-29
47. C2H3+O2<=>CH2O+HCO                                1.70E+29   -5.3     6503.1
48. C2H3+O2<=>CH2CHO+O                                7.00E+14   -0.6     5262.4
49. C2H3+O2<=>C2H2+HO2                                5.19E+15   -1.3     3312.6
50. C2H2+O<=>HCCO+H                                   4.00E+14    0.0    10659.7
51. C2H2+OH<=>CH2CO+H                                 1.90E+07    1.7      999.0
52. CH2CO+H<=>CH3+CO                                  1.50E+09    1.4     2688.8
53. CH2CO+O<=>T-CH2+CO2                               2.00E+13    0.0     2294.5
54. CH2CO+CH3<=>C2H5+CO                               9.00E+10    0.0        0.0
55. HCCO+O2<=>2CO+OH                                  2.88E+07    1.7     1001.4
56. CH2OH+H<=>CH2O+H2                                 3.00E+13    0.0        0.0
57. CH2OH+H<=>CH3+OH                                  2.50E+17   -0.9     5126.9
```

```
58. CH2OH+M<=>CH2O+H+M                              5.00E+13    0.0    25119.5
    AR              Enhanced by    7.000E-01
    H2              Enhanced by    2.000E+00
    H2O             Enhanced by    6.000E+00
    CO              Enhanced by    1.500E+00
    CO2             Enhanced by    2.000E+00
    CH4             Enhanced by    2.000E+00
59. CH2CO+OH<=>CH2OH+CO                            1.02E+13    0.0        0.0
60. CH2CHO<=>CH2CO+H                               1.05E+37   -7.2    44340.3
61. CH2CHO+O2<=>CH2O+CO+OH                         3.00E+10    0.0        0.0
62. CH2CHO+HO2<=>CH2O+HCO+OH                       7.00E+12    0.0        0.0
63. CH2CHO+HO2<=>CH3CHO+O2                         3.00E+12    0.0        0.0
64. CH3CO(+M)<=>CH3+CO(+M)                         3.00E+12    0.0    16700.0
    AR              Enhanced by    7.000E-01
    H2              Enhanced by    2.000E+00
    H2O             Enhanced by    6.000E+00
    CO              Enhanced by    1.500E+00
    CO2             Enhanced by    2.000E+00
    CH4             Enhanced by    2.000E+00
    Low pressure limit:  0.12000E+16  0.00000E+00  0.12500E+05
    TROE centering:      0.10000E+01  0.10000E+01  0.10000E+08  0.10000E+08
65. CH3CHO+OH<=>CH3CO+H2O                          3.37E+12    0.0     -620.0
66. C2H5+HO2<=>CH3CH2O+OH                          4.00E+13    0.0        0.0
67. CH3CH2O+M<=>CH3CHO+H+M                         5.60E+34   -5.9    25300.0
    AR              Enhanced by    7.000E-01
    H2              Enhanced by    2.000E+00
    H2O             Enhanced by    6.000E+00
    CO              Enhanced by    1.500E+00
    CO2             Enhanced by    2.000E+00
    CH4             Enhanced by    2.000E+00
68. CH3CH2O+M<=>CH3+CH2O+M                         5.35E+37   -7.0    23800.0
    AR              Enhanced by    7.000E-01
    H2              Enhanced by    2.000E+00
    H2O             Enhanced by    6.000E+00
    CO              Enhanced by    1.500E+00
    CO2             Enhanced by    2.000E+00
    CH4             Enhanced by    2.000E+00
69. CH3+C2H2<=>C3H4+H                              2.56E+09    1.1    13643.9
70. C3H4+H(+M)<=>C3H5(+M)                          4.00E+13    0.0        0.0
    Low pressure limit:  0.30000E+25 -0.20000E+01  0.00000E+00
    TROE centering:      0.80000E+00  0.10000E+31  0.10000E-29
71. C3H5+H<=>C3H4+H2                               1.80E+13    0.0        0.0
72. C3H6+OH<=>C3H5+H2O                             3.10E+06    2.0     -298.3
73. C3H6+O<=>CH2CO+CH3+H                           1.20E+08    1.6      327.4
74. C3H6+H<=>C3H5+H2                               1.70E+05    2.5     2492.8
75. C3H5+H(+M)<=>C3H6(+M)                          2.00E+14    0.0        0.0
    AR              Enhanced by    7.000E-01
    H2              Enhanced by    2.000E+00
    H2O             Enhanced by    6.000E+00
    CO              Enhanced by    1.500E+00
    CO2             Enhanced by    2.000E+00
    CH4             Enhanced by    2.000E+00
    C2H6            Enhanced by    3.000E+00
    Low pressure limit:  0.13300E+61 -0.12000E+02  0.59680E+04
    TROE centering:      0.20000E-01  0.10970E+04  0.10970E+04  0.68600E+04
76. C3H5+HO2<=>C3H6+O2                             2.66E+12    0.0        0.0
77. C3H5+HO2<=>OH+C2H3+CH2O                        3.00E+12    0.0        0.0
```

```
78. C2H3+CH3(+M)<=>C3H6(+M)                          2.50E+13    0.0        0.0
    AR              Enhanced by    7.000E-01
    H2              Enhanced by    2.000E+00
    H2O             Enhanced by    6.000E+00
    CO              Enhanced by    1.500E+00
    CO2             Enhanced by    2.000E+00
    CH4             Enhanced by    2.000E+00
    C2H6            Enhanced by    3.000E+00
    Low pressure limit:  0.42700E+59 -0.11940E+02  0.97705E+04
    TROE centering:      0.17500E+00  0.13410E+04  0.60000E+05  0.10140E+05
79. C3H6+H<=>C2H4+CH3                               1.60E+22   -2.4    11185.5
80. C3H6+H(+M)<=>I-C3H7(+M)                         1.33E+13    0.0     1560.7
    AR              Enhanced by    7.000E-01
    H2              Enhanced by    2.000E+00
    H2O             Enhanced by    6.000E+00
    CO              Enhanced by    1.500E+00
    CO2             Enhanced by    2.000E+00
    CH4             Enhanced by    2.000E+00
    C2H6            Enhanced by    3.000E+00
    Low pressure limit:  0.87000E+43 -0.75000E+01  0.47323E+04
    TROE centering:      0.10000E+01  0.10000E+04  0.64540E+03  0.68440E+04
81. C4H8<=>C3H5+CH3                                 1.00E+16    0.0    72896.8
82. C4H8+H<=>H2+C2H3+C2H4                           6.60E+05    2.5     6763.9
83. C4H6+H=>C2H3+C2H4                               5.00E+11    0.0        0.0
84. C4H6+H=>H2+C2H2+C2H3                            6.30E+10    0.7     6001.4
85. C4H6+OH=>HCO+H+C3H5                             5.00E+12    0.0        0.0
86. C4H6+CH3=>CH4+C2H2+C2H3                         7.00E+13    0.0    18413.0
87. C5H10<=>C3H5+C2H5                               1.00E+16    0.0    72896.8
88. C4H8+H<=>C3H6+CH3                               7.23E+12    0.0     1290.6

NOTE:  A units mole-cm-sec-K, E units cal/mole
```

Appendix C. Comparison of Results Obtained from Solutions to Various Opposed-Flow Diffusion Flame Problems Produced with the San Diego Mechanism and with A45.10_04

This report summarizes an evaluation of the potential to create skeletal finite-rate chemical kinetics mechanisms for modeling reacting flows in solid-fuel ramjet combustors based on a trial mechanism method (TMM) implementation in which reactions were eliminated from the San Diego (SD) mechanism based on analyzing parameter values derived from solutions to opposed-flow diffusion flame (OFDF) problems. The evaluation included comparing temperature (T) and heat release rate per unit mass ($\dot{q}_{mass}$) versus distance plots obtained from solutions to 18 different OFDF problems produced with the SD mechanism and with a skeletal mechanism (A45.10_04) derived from it. The set included nine different combinations of pressure (P) and velocity of air at the oxidizer inlet (V_{ox}). For each P-V_{ox} combination, two problems were set up and solved: one with the temperature at the fuel inlet (T_{fuel}) equal to 500 or 525 K, and the other with it equal to 650 K. Since all plots obtained from T_{fuel} = 650 K simulations were qualitatively similar to those obtained from their T_{fuel} = 500 (or 525) K counterpart, only the latter were presented and discussed in the main body of the report. For reference, plots obtained from the solutions to the T_{fuel} = 650 K problems are presented herein (Figs. C-1 through C-9).

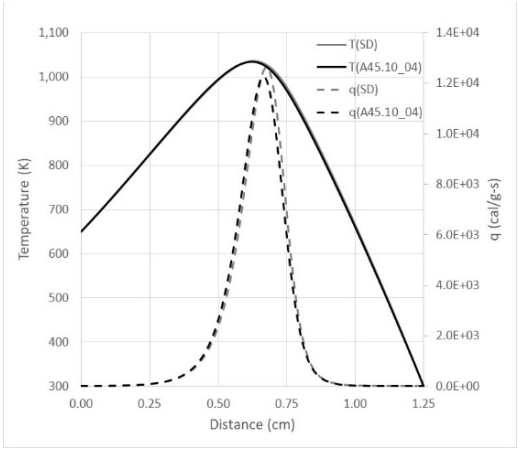

Fig. C-1 Comparison of results produced with the SD mechanism and with A45.10_04 for OFDF simulation 10: P = 0.4 atm, V_{ox} = 2 cm/s, T_{fuel} = 650 K

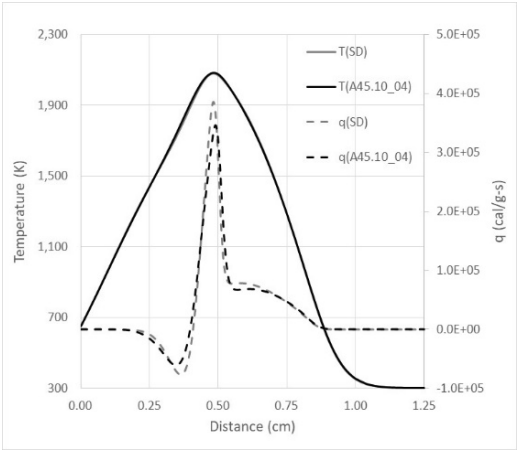

Fig. C-2 Comparison of results produced with the SD mechanism and with A45.10_04 for OFDF simulation 11: P = 0.4 atm, V_{ox} = 17 cm/s, T_{fuel} = 650 K

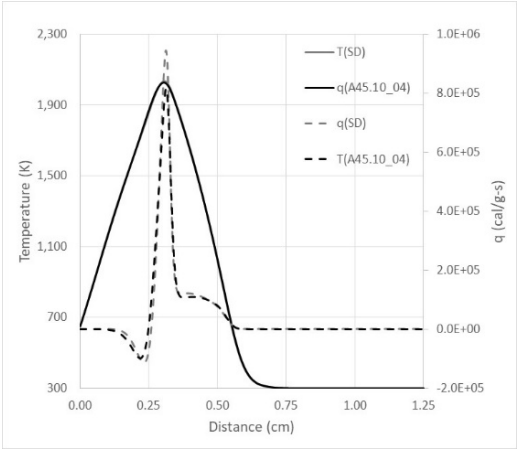

Fig. C-3 Comparison of results produced with the SD mechanism and with A45.10_04 for OFDF simulation 12: P = 0.4 atm, V_{ox} = 54 cm/s, T_{fuel} = 650 K

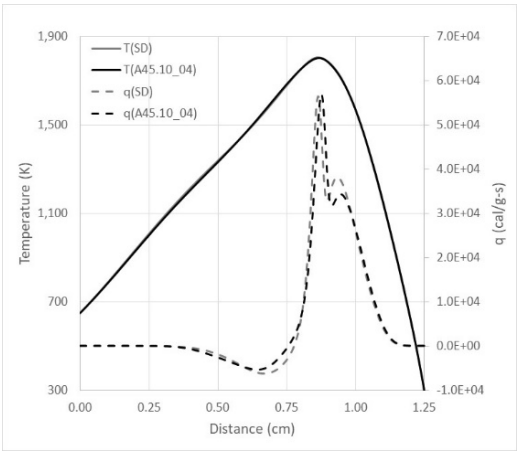

Fig. C-4 Comparison of results produced with the SD mechanism and with A45.10_04 for OFDF simulation 13: P = 1.0 atm, V_{ox} = 2 cm/s, T_{fuel} = 650 K

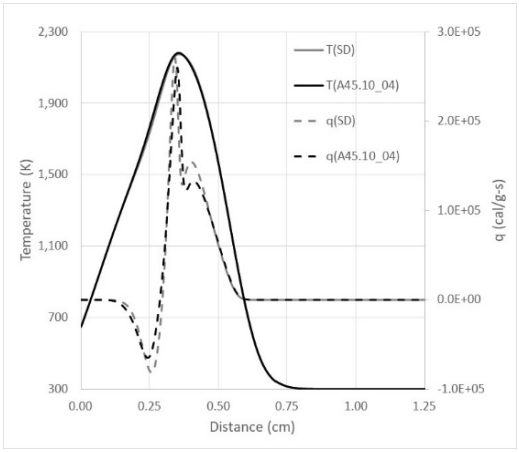

Fig. C-5 Comparison of results produced with the SD mechanism and with A45.10_04 for OFDF simulation 14: P = 1.0 atm, V_{ox} = 17 cm/s, T_{fuel} = 650 K

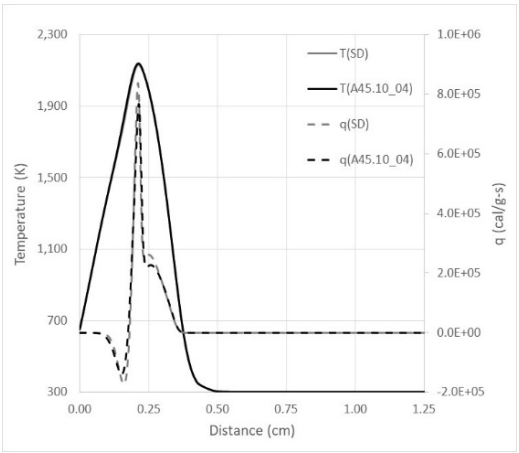

Fig. C-6 Comparison of results produced with the SD mechanism and with A45.10_04 for OFDF simulation 15: P = 1.0 atm, V_{ox} = 54 cm/s, T_{fuel} = 650 K

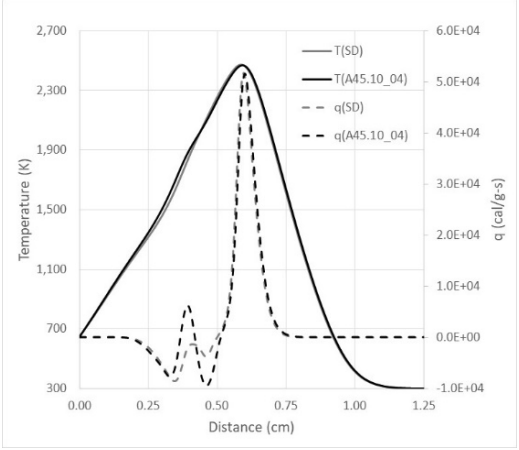

Fig. C-7 Comparison of results produced with the SD mechanism and with A45.10_04 for OFDF simulation 16: P = 6.2 atm, V_{ox} = 1 cm/s, T_{fuel} = 650 K

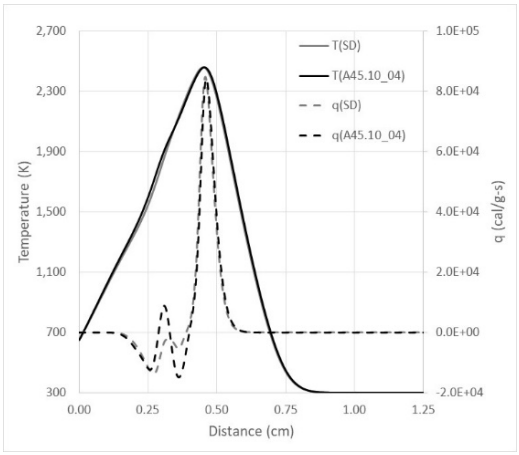

Fig. C-8 Comparison of results produced with the SD mechanism and with A45.10_04 for OFDF simulation 17: P = 6.2 atm, V_{ox} = 2 cm/s, T_{fuel} = 650 K

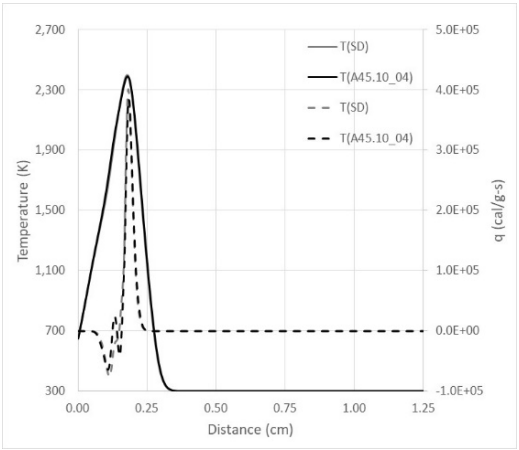

Fig. C-9 Comparison of results produced with the SD mechanism and with A45.10_04 for OFDF simulation 18: P = 6.2 atm, V_{ox} = 17 cm/s, T_{fuel} = 650 K

Appendix D. Summary of Evaluations of Trial Reaction Eliminations from A45.10_03

Table D-1 summarizes the reasons reactions were not permanently eliminated from the skeletal mechanism that was the direct precursor of A45.10_04, namely A45.10_03. It was created from a log file generated during the course of the process.

Table D-1 Reasons reactions in A45.10_03 were retained or permanently eliminated

```
************************************************
* :::::: REACTION   81   CH3O+M<=>CH2O+H+M
* ++++RETAINED+++     Required by condition 1
* NMAX =  500 was exceeded.
* TOTAL ANALYSIS TIME (sec):   246.3712
************************************************
* :::::: REACTION   93   C2H4OOH<=>C2H4+HO2
* ++++RETAINED+++     Required by condition 1
* Tmax is off by :-30.9 K
* d(Tmax) error  :   -5.1%
* dT/dx error      :   -1.7%
* TOTAL ANALYSIS TIME (sec):    14.5554
************************************************
* :::::: REACTION   17   2HO2<=>H2O2+O2
* ++++RETAINED+++     Required by condition 1
* Tmax is off by : 64.6 K
* d(Tmax) error  :   17.3%
* dT/dx error      :   -0.5%
* TOTAL ANALYSIS TIME (sec):    26.9906
************************************************
* :::::: REACTION  109   C2H3+O2<=>CH2O+HCO
* ++++RETAINED+++     Required by condition 1
* Tmax is off by : 48.5 K
* d(Tmax) error  :   17.3%
* dT/dx error      :    1.4%
* TOTAL ANALYSIS TIME (sec):    45.0299
************************************************
* :::::: REACTION  117   CH2CO+H<=>CH3+CO
* ++++RETAINED+++     Required by condition 1
* NMAX =  500 was exceeded.
* TOTAL ANALYSIS TIME (sec):    60.3518
************************************************
* :::::: REACTION   98   C2H4+OH<=>C2H3+H2O
* ++++RETAINED+++     Required by condition 1
* Tmax is off by : >100 K
* d(Tmax) error  : >100%
* dT/dx error      : >100%
* TOTAL ANALYSIS TIME (sec):   279.3278
************************************************
* :::::: REACTION  153   CH2CHO+HO2<=>CH2O+HCO+OH
* ++++RETAINED+++     Required by condition 1
* Tmax is off by : >100 K
* d(Tmax) error  : >100%
* dT/dx error      : >100%
* TOTAL ANALYSIS TIME (sec):   165.9255
************************************************
```

```
************************************************
* :::::: REACTION  306   C5H10<=>C3H5+C2H5
* ++++RETAINED+++     Required by condition 9
* NMAX =  500 was exceeded.
* TOTAL ANALYSIS TIME (sec):    69.0845
************************************************
* :::::: REACTION  222   C3H5+H(+M)<=>C3H6(+M)
* ++++RETAINED+++     Required by condition 1
* Tmax is off by :-35.9 K
* d(Tmax) error  :   -6.3%
* dT/dx error    :   -1.1%
* TOTAL ANALYSIS TIME (sec):     3.3069
************************************************
* :::::: REACTION  111   C2H3+O2<=>C2H2+HO2
* ++++RETAINED+++     Required by condition 1
* Tmax is off by : 55.1 K
* d(Tmax) error  :   13.0%
* dT/dx error    :    2.9%
* TOTAL ANALYSIS TIME (sec):    47.5347
************************************************
* :::::: REACTION    3   H2+OH<=>H2O+H
* ++++RETAINED+++     Required by condition 1
* Tmax is off by :-10.7 K
* d(Tmax) error  :   -2.0%
* dT/dx error    :    0.4%
* TOTAL ANALYSIS TIME (sec):    19.1678
************************************************
* :::::: REACTION  158   CH3CHO+OH<=>CH3CO+H2O
* ++++RETAINED+++     Required by condition 1
* Tmax is off by :-20.5 K
* d(Tmax) error  :   -3.9%
* dT/dx error    :   -0.0%
* TOTAL ANALYSIS TIME (sec):     5.6456
************************************************
* :::::: REACTION   13   HO2+O<=>OH+O2
* ++++RETAINED+++     Required by condition 1
* Tmax is off by :-14.7 K
* d(Tmax) error  :   -2.0%
* dT/dx error    :    0.3%
* TOTAL ANALYSIS TIME (sec):     3.3419
************************************************
* :::::: REACTION  263   C4H8+H<=>H2+C2H3+C2H4
* ++++RETAINED+++     Required by condition 1
* Tmax is off by : >100 K
* d(Tmax) error  : >100%
* dT/dx error    : >100%
* TOTAL ANALYSIS TIME (sec):   156.3865
************************************************
* :::::: REACTION  262   C4H8<=>C3H5+CH3
* ++++RETAINED+++     Required by condition 1
* Tmax is off by : 56.1 K
* d(Tmax) error  :   31.2%
* dT/dx error    :  -11.0%
* TOTAL ANALYSIS TIME (sec):    37.2587
************************************************
```

```
************************************************
* :::::: REACTION  272   C4H6+H=>C2H3+C2H4
* ++++RETAINED+++     Required by condition 1
* NMAX =  500 was exceeded.
* TOTAL ANALYSIS TIME (sec):    70.5138
************************************************
* :::::: REACTION   19   H2O2+H<=>HO2+H2
* ++++RETAINED+++     Required by condition 1
* Tmax is off by :-16.6 K
* d(Tmax) error  :   -3.9%
* dT/dx error    :    0.0%
* TOTAL ANALYSIS TIME (sec):     3.0037
************************************************
* :::::: REACTION  315   C4H8+H<=>C3H6+CH3
* ++++RETAINED+++     Required by condition 1
* Tmax is off by : 76.6 K
* d(Tmax) error  :   22.0%
* dT/dx error    :   -2.5%
* TOTAL ANALYSIS TIME (sec):    89.9371
************************************************
* :::::: REACTION   67   T-CH2+O2<=>CO2+H2
* ++++RETAINED+++     Required by condition 1
* Tmax is off by :-17.9 K
* d(Tmax) error  :   -3.9%
* dT/dx error    :    0.0%
* TOTAL ANALYSIS TIME (sec):     3.0244
************************************************
* :::::: REACTION  113   C2H2+O<=>T-CH2+CO
* REACTION  113   PERMANENTLY ELIMINATED
* TOTAL ANALYSIS TIME (sec):    80.0152
************************************************
* :::::: REACTION  110   C2H3+O2<=>CH2CHO+O
* ++++RETAINED+++     Required by condition 1
* NMAX =  500 was exceeded.
* TOTAL ANALYSIS TIME (sec):   134.1370
************************************************
* :::::: REACTION   20   H2O2+H<=>H2O+OH
* ++++RETAINED+++     Required by condition 1
* Tmax is off by : >100 K
* d(Tmax) error  : >100%
* dT/dx error    : >100%
* TOTAL ANALYSIS TIME (sec):   162.7765
************************************************
* :::::: REACTION  220   C3H6+O<=>CH2CO+CH3+H
* ++++RETAINED+++     Required by condition 1
* NMAX =  500 was exceeded.
* TOTAL ANALYSIS TIME (sec):    37.8723
************************************************
* :::::: REACTION   14   HO2+OH<=>H2O+O2
* ++++RETAINED+++     Required by condition 18
* NMAX =  500 was exceeded.
* TOTAL ANALYSIS TIME (sec):   230.5622
************************************************
```

```
************************************************
* :::::: REACTION  154   CH2CHO+HO2<=>CH3CHO+O2
* ++++RETAINED+++     Required by condition 1
* NMAX =  500 was exceeded.
* TOTAL ANALYSIS TIME (sec):    42.2218
************************************************
* :::::: REACTION  102   C2H4+O2<=>C2H3+HO2
* ++++RETAINED+++     Required by condition 1
* Tmax is off by :-38.6 K
* d(Tmax) error  :   -9.6%
* dT/dx error      :    3.5%
* TOTAL ANALYSIS TIME (sec):    17.5456
************************************************
* :::::: REACTION  155   CH2CHO<=>CH3+CO
* REACTION 155 PERMANENTLY ELIMINATED
* TOTAL ANALYSIS TIME (sec):    96.7355
************************************************
* :::::: REACTION   22   H2O2+OH<=>H2O+HO2
* ++++RETAINED+++     Required by condition 1
* Tmax is off by :-18.3 K
* d(Tmax) error  :   -2.0%
* dT/dx error      :   -0.3%
* TOTAL ANALYSIS TIME (sec):    15.1286
************************************************
* :::::: REACTION  120   CH2CO+CH3<=>C2H5+CO
* ++++RETAINED+++     Required by condition 1
* NMAX =  500 was exceeded.
* TOTAL ANALYSIS TIME (sec):   282.9466.
************************************************
* :::::: REACTION   21   H2O2+OH<=>H2O+HO2
* ++++RETAINED+++     Required by condition 1
* Tmax is off by :-13.6 K
* d(Tmax) error  :   -2.0%
* dT/dx error      :    0.1%
* TOTAL ANALYSIS TIME (sec):    25.9227
************************************************
* :::::: REACTION   18   2HO2<=>H2O2+O2
* ++++RETAINED+++     Required by condition 1
* Tmax is off by : 65.6 K
* d(Tmax) error  :   22.0%
* dT/dx error      :   -3.3%
* TOTAL ANALYSIS TIME (sec):    14.7664
************************************************
* :::::: REACTION   42   CH4+OH<=>H2O+CH3
* ++++RETAINED+++     Required by condition 2
* Tmax is off by :-30.3 K
* d(Tmax) error  :   -3.4%
* dT/dx error      :    0.1%
* TOTAL ANALYSIS TIME (sec):    26.0025
************************************************
```

```
************************************************
* :::::: REACTION  203   CH3+C2H2<=>C3H4+H
* ++++RETAINED+++     Required by condition 4
* Tmax is off by : 10.3 K
* d(Tmax) error  :    0.2%
* dT/dx error    :    2.1%
* TOTAL ANALYSIS TIME (sec):    20.2923
************************************************
* :::::: REACTION  137   CH2CO+OH<=>CH2OH+CO
* ++++RETAINED+++     Required by condition 1
* NMAX =  500 was exceeded
* TOTAL ANALYSIS TIME (sec):    32.3429
************************************************
* :::::: REACTION   51   CH3+HO2<=>CH3O+OH
* ++++RETAINED+++     Required by condition 1
* Tmax is off by : >100 K
* d(Tmax) error  : >100%
* dT/dx error    : >100%
* TOTAL ANALYSIS TIME (sec):   145.6540
************************************************
* :::::: REACTION  240   C3H6+H(+M)<=>I-C3H7(+M)
* ++++RETAINED+++     Required by condition 1
* NMAX =  500 was exceeded.
* TOTAL ANALYSIS TIME (sec):    54.4966
************************************************
* :::::: REACTION  135   CH2OH+M<=>CH2O+H+M
* ++++RETAINED+++     Required by condition 1
* NMAX =  500 was exceeded.
* TOTAL ANALYSIS TIME (sec):   292.7263
************************************************
* :::::: REACTION  146   CH2CHO<=>CH2CO+H
* ++++RETAINED+++     Required by condition 1
* Tmax is off by :-33.0 K
* d(Tmax) error  :   -8.0%
* dT/dx error    :   -0.1%
* TOTAL ANALYSIS TIME (sec):     2.4048
************************************************
* :::::: REACTION  210   C3H5+H<=>C3H4+H2
* ++++RETAINED+++     Required by condition 1
* Tmax is off by :-12.2 K
* d(Tmax) error  :   -2.0%
* dT/dx error    :    0.5%
* TOTAL ANALYSIS TIME (sec):    15.8326
************************************************
* :::::: REACTION  124   HCCO+O2<=>2CO+OH
* ++++RETAINED+++     Required by condition 1
* Tmax is off by : >100 K
* d(Tmax) error  : >100%
* dT/dx error    : >100%
* TOTAL ANALYSIS TIME (sec):   172.5930
************************************************
```

```
************************************************
* :::::: REACTION  274   C4H6+OH=>HCO+H+C3H5
* ++++RETAINED+++     Required by condition 1
* Tmax is off by : >100 K
* d(Tmax) error  : >100%
* dT/dx error      : >100%
* TOTAL ANALYSIS TIME (sec):    39.2637
************************************************
* :::::: REACTION   46   CH3+H<=>T-CH2+H2
* ++++RETAINED+++     Required by condition 3
* Tmax is off by :-11.5 K
* d(Tmax) error  :   -0.0%
* dT/dx error      :   -0.4%
* TOTAL ANALYSIS TIME (sec):    33.6818
************************************************
* :::::: REACTION   11   HO2+H<=>H2+O2
* ++++RETAINED+++     Required by condition 1
* Tmax is off by :-23.0 K
* d(Tmax) error  :   -3.9%
* dT/dx error      :   -0.4%
* TOTAL ANALYSIS TIME (sec):    13.0991
************************************************
* :::::: REACTION  187   C2H5+HO2<=>CH3CH2O+OH
* ++++RETAINED+++     Required by condition 1
* Tmax is off by : >100 K
* d(Tmax) error  : >100%
* dT/dx error      : >100%
* TOTAL ANALYSIS TIME (sec):   229.0458
************************************************
* :::::: REACTION   99   C2H4+O<=>CH3+HCO
* ++++RETAINED+++     Required by condition 1
* NMAX =  500 was exceeded.
* TOTAL ANALYSIS TIME (sec):    64.6640
************************************************
* :::::: REACTION   70   C2H2+HO2<=>CHCHO+OH
* ++++RETAINED+++     Required by condition 1
* NMAX =  500 was exceeded.
* TOTAL ANALYSIS TIME (sec):   255.4790
************************************************
* :::::: REACTION  132   CH2OH+H<=>CH3+OH
* ++++RETAINED+++     Required by condition 1
* NMAX =  500 was exceeded.
* TOTAL ANALYSIS TIME (sec):   215.3322
************************************************
* :::::: REACTION  112   C2H2+O<=>HCCO+H
* ++++RETAINED+++     Required by condition 1
* Tmax is off by : >100 K
* d(Tmax) error  : >100%
* dT/dx error      : >100%
* TOTAL ANALYSIS TIME (sec):   257.0043
************************************************
* :::::: REACTION   37   CH2O+O<=>HCO+OH
* ++++RETAINED+++     Required by condition 1
* NMAX =  500 was exceeded.
* TOTAL ANALYSIS TIME (sec):    30.8075
************************************************
```

```
************************************************
* :::::: REACTION  209   C3H4+H(+M)<=>C3H5(+M)
* ++++RETAINED+++     Required by condition 4
* NMAX =  500 was exceeded.
* TOTAL ANALYSIS TIME (sec):    54.1464
************************************************
* :::::: REACTION   92   C2H5+O2<=>C2H4OOH
* ++++RETAINED+++     Required by condition 1
* Tmax is off by :-31.3 K
* d(Tmax) error  :   -3.9%
* dT/dx error    :   -1.6%
* TOTAL ANALYSIS TIME (sec):    15.2679
************************************************
* :::::: REACTION   49   CH3+O<=>CH2O+H
* ++++RETAINED+++     Required by condition 11
* Tmax is off by : 10.1 K
* d(Tmax) error  :    0.0%
* dT/dx error    :   -0.4%
* TOTAL ANALYSIS TIME (sec):    54.7807
************************************************
* :::::: REACTION  273   C4H6+H=>H2+C2H2+C2H3
* ++++RETAINED+++     Required by condition 1
* Tmax is off by :-29.5 K
* d(Tmax) error  :   -9.6%
* dT/dx error    :    5.2%
* TOTAL ANALYSIS TIME (sec):     3.0315
************************************************
* :::::: REACTION  219   C3H6+OH<=>C3H5+H2O
* ++++RETAINED+++     Required by condition 1
* Tmax is off by :-22.8 K
* d(Tmax) error  :   -3.9%
* dT/dx error    :   -0.7%
* TOTAL ANALYSIS TIME (sec):     2.8395
************************************************
* :::::: REACTION   56   H+CH3(+M)<=>CH4(+M)
* ++++RETAINED+++     Required by condition 2
* Tmax is off by :-10.5 K
* d(Tmax) error  :   -0.5%
* dT/dx error    :   -0.7%
* TOTAL ANALYSIS TIME (sec):    15.8650
************************************************
* :::::: REACTION  189   CH3CH2O+M<=>CH3+CH2O+M
* ++++RETAINED+++     Required by condition 1
* NMAX =  500 was exceeded.
* TOTAL ANALYSIS TIME (sec):    40.6019
************************************************
* :::::: REACTION   97   C2H4+H<=>C2H3+H2
* ++++RETAINED+++     Required by condition 1
* Tmax is off by :-11.6 K
* d(Tmax) error  :   -2.0%
* dT/dx error    :    0.6%
* TOTAL ANALYSIS TIME (sec):    16.9093
************************************************
```

```
************************************************
* :::::: REACTION   38   CH2O+OH<=>HCO+H2O
* ++++RETAINED+++     Required by condition 1
* Tmax is off by : 30.3 K
* d(Tmax) error  :    9.2%
* dT/dx error    :   -1.0%
* TOTAL ANALYSIS TIME (sec):    47.7037
************************************************
* :::::: REACTION  118   CH2CO+O<=>T-CH2+CO2
* ++++RETAINED+++     Required by condition 1
* NMAX =  500 was exceeded.
* TOTAL ANALYSIS TIME (sec):   296.3304
************************************************
* :::::: REACTION  157   CH3CO(+M)<=>CH3+CO(+M)
* Simulation completed    1   -2  233 175441.924
* ++++RETAINED+++     Required by condition 1
* NMAX =  500 was exceeded.
* TOTAL ANALYSIS TIME (sec):   175.4420
************************************************
* :::::: REACTION  226   C3H6+H<=>C2H4+CH3
* ++++RETAINED+++     Required by condition 1
* Tmax is off by : 11.7 K
* d(Tmax) error  :    3.7%
* dT/dx error    :    1.6%
* TOTAL ANALYSIS TIME (sec):     3.1409
************************************************
* :::::: REACTION  101   2C2H4<=>C2H3+C2H5
* ++++RETAINED+++     Required by condition 1
* Tmax is off by : 47.6 K
* d(Tmax) error  :    9.2%
* dT/dx error    :    3.5%
* TOTAL ANALYSIS TIME (sec):    51.4525
************************************************
* :::::: REACTION  151   CH2CHO+O2<=>CH2O+CO+OH
* ++++RETAINED+++     Required by condition 1
* Tmax is off by : >100 K
* d(Tmax) error  : >100%
* dT/dx error    : >100%
* TOTAL ANALYSIS TIME (sec):   122.0395
************************************************
* :::::: REACTION  275   C4H6+CH3=>CH4+C2H2+C2H3
* ++++RETAINED+++     Required by condition 1
* NMAX =  500 was exceeded.
* TOTAL ANALYSIS TIME (sec):   283.1842
************************************************
* :::::: REACTION   71   CHCHO+O2=CH2O+CO+O
* ++++RETAINED+++     Required by condition 1
* NMAX =  500 was exceeded.
* TOTAL ANALYSIS TIME (sec):   275.3965
************************************************
* :::::: REACTION   25   CO+OH<=>CO2+H
* ++++RETAINED+++     Required by condition 2
* NMAX =  500 was exceeded.
* TOTAL ANALYSIS TIME (sec):    31.4421
************************************************
```

```
************************************************
* :::::: REACTION   16   2OH(+M)<=>H2O2(+M)
* ++++RETAINED+++     Required by condition 1
* NMAX =  500 was exceeded.
* TOTAL ANALYSIS TIME (sec):   244.0181
************************************************
* :::::: REACTION  107   C2H3+H<=>C2H2+H2
* ++++RETAINED+++     Required by condition 2
* Tmax is off by :-22.7 K
* d(Tmax) error  :    0.0%
* dT/dx error    :   -2.8%
* TOTAL ANALYSIS TIME (sec):    16.4101
************************************************
* :::::: REACTION   28   HCO+M<=>CO+H+M
* ++++RETAINED+++     Required by condition 1
* Tmax is off by :-23.4 K
* d(Tmax) error  :   -3.9%
* dT/dx error    :   -3.4
* TOTAL ANALYSIS TIME (sec):     7.7190
************************************************
* :::::: REACTION  131   CH2OH+H<=>CH2O+H2
* ++++RETAINED+++     Required by condition 1
* Tmax is off by :-18.4 K
* d(Tmax) error  :   -3.9%
* dT/dx error    :    0.0%
* TOTAL ANALYSIS TIME (sec):    15.5637
************************************************
* :::::: REACTION  188   CH3CH2O+M<=>CH3CHO+H+M
* ++++RETAINED+++     Required by condition 1
* Tmax is off by : >100 K
* d(Tmax) error  : >100%
* dT/dx error    : >100%
* TOTAL ANALYSIS TIME (sec):   172.3918
************************************************
* :::::: REACTION   36   CH2O+H<=>HCO+H2
* ++++RETAINED+++     Required by condition 1
* Tmax is off by :-49.0 K
* d(Tmax) error  :   -9.6%
* dT/dx error    :   -2.4%
* TOTAL ANALYSIS TIME (sec):     3.6769
************************************************
* :::::: REACTION  108   C2H3(+M)<=>C2H2+H(+M)
* ++++RETAINED+++     Required by condition 2
* Tmax is off by : 66.9 K
* d(Tmax) error  :    1.5%
* dT/dx error    :    7.1%
* TOTAL ANALYSIS TIME (sec):    16.5433
************************************************
* :::::: REACTION   34   HCO+CH3<=>CO+CH4
* ++++RETAINED+++     Required by condition 1
* Tmax is off by :-16.2 K
* d(Tmax) error  :   -2.0%
* dT/dx error    :   -0.1%
* ANALYSIS TOTAL TIME (sec) WAS :     3.0327
************************************************
```

```
************************************************
* :::::: REACTION  115   C2H2+OH<=>CH2CO+H
* ++++RETAINED+++     Required by condition 2
* Tmax is off by :-11.2 K
* d(Tmax) error  :    2.7%
* dT/dx error      :   -6.0%
* TOTAL ANALYSIS TIME (sec):    13.7495
************************************************
* :::::: REACTION    4   H2O+O<=>2OH
* ++++RETAINED+++     Required by condition 2
* Tmax is off by : >100 K
* d(Tmax) error  :   -4.4%
* dT/dx error       :   -4.3%
* TOTAL ANALYSIS TIME (sec):    27.9168
************************************************
* :::::: REACTION    6   H+OH+M<=>H2O+M
* ++++RETAINED+++     Required by condition 2
* Tmax is off by :-22.3 K
* d(Tmax) error  :   -1.5%
* dT/dx error      :   -0.4%
* TOTAL ANALYSIS TIME (sec):    17.5550
************************************************
* :::::: REACTION   33   HCO+O2<=>CO+HO2
* ++++RETAINED+++     Required by condition 1
* Tmax is off by : >100 K
* d(Tmax) error  : -18.6%
* dT/dx error      : -23.0%
* TOTAL ANALYSIS TIME (sec):    83.9251
************************************************
* :::::: REACTION   10   HO2+H<=>2OH
* ++++RETAINED+++     Required by condition 1
* NMAX =  500 was exceeded.
* TOTAL ANALYSIS TIME (sec):    27.2721
************************************************
* :::::: REACTION    1   H+O2<=>OH+O
* ++++RETAINED+++     Required by condition 1
* NMAX =  500 was exceeded.
* TOTAL ANALYSIS TIME (sec):   222.5028
************************************************
* :::::: REACTION   50   CH3+T-CH2<=>C2H4+H
* ++++RETAINED+++     Required by condition 10
* NMAX =  500 was exceeded.
* TOTAL ANALYSIS TIME (sec):   112.4409
************************************************
* :::::: REACTION  221   C3H6+H<=>C3H5+H2
* ++++RETAINED+++     Required by condition 1
* Tmax is off by :-23.9 K
* d(Tmax) error  :   -3.9
* dT/dx error      :   -0.6%
* TOTAL ANALYSIS TIME (sec):     3.1049
************************************************
```

```
************************************************
* :::::: REACTION   96   C2H5(+M)<=>C2H4+H(+M)
* ++++RETAINED+++     Required by condition 1
* Tmax is off by : >100 K
* d(Tmax) error  : >100%
* dT/dx error      : >100%
* TOTAL ANALYSIS TIME (sec):   257.4351
************************************************
* :::::: REACTION    9   H+O2(+M)<=>HO2(+M)
* ++++RETAINED+++     Required by condition 2
* Tmax is off by :-24.6 K
* d(Tmax) error  :   -0.5%
* dT/dx error      :   -2.0%
* TOTAL ANALYSIS TIME (sec):    17.0912
************************************************
* :::::: REACTION   68   T-CH2+O2<=>CO+OH+H
* Simulation completed    1    0  227 165635.259
* ++++RETAINED+++     Required by condition 1
* Tmax is off by : >100 K
* d(Tmax) error  : >100%
* dT/dx error      : >100%
* TOTAL ANALYSIS TIME (sec):   165.6353
************************************************
* :::::: REACTION  224   C3H5+HO2<=>OH+C2H3+CH2O
* ++++RETAINED+++     Required by condition 1
* Tmax is off by : >100 K
* d(Tmax) error  : >100%
* dT/dx error      : >100%
* TOTAL ANALYSIS TIME (sec):    85.5010
************************************************
* :::::: REACTION  225   C2H3+CH3(+M)<=>C3H6(+M)
* ++++RETAINED+++     Required by condition 1
* Tmax is off by :-24.0 K
* d(Tmax) error  :   -5.1%
* dT/dx error      :   -0.1%
* TOTAL ANALYSIS TIME (sec):     3.1037
************************************************
* :::::: REACTION  223   C3H5+HO2<=>C3H6+O2
* ++++RETAINED+++     Required by condition 1
* Tmax is off by : 64.0 K
* d(Tmax) error  :   18.5%
* dT/dx error      :    0.6%
* TOTAL ANALYSIS TIME (sec):    35.5288
************************************************
* :::::: REACTION   26   CO+HO2<=>CO2+OH
* ++++RETAINED+++     Required by condition 1
* Tmax is off by : >100 K
* d(Tmax) error  : >100%
* dT/dx error      : >100%
* TOTAL ANALYSIS TIME (sec):   271.4313
************************************************
```

```
************************************************
* :::::: REACTION   40   CH2O+HO2<=>HCO+H2O2
* ++++RETAINED+++     Required by condition 1
* Tmax is off by : >100 K
* d(Tmax) error  : >100%
* dT/dx error       : >100%
* TOTAL ANALYSIS TIME (sec):   181.3134
************************************************
 No. of reactions :   88
 No. of species   :   38
 Mechanism        :   36
 Input only       :    2
 Enhanced 3B only :    2  HE C2H6
```

List of Symbols, Abbreviations, and Acronyms

1-D	one-dimensional
ARL	Army Research Laboratory
CCDC	US Army Combat Capabilities Development Command
CFD	computational fluid dynamics
DoD	Department of Defense
DSRC	DoD Shared Resource Center
HPC	High Performance Computing
HR	homogeneous reactor
HTPB	hydroxyl-terminated polybutadiene
MAD	maximum allowable deviation
O/F	oxidizer-to-fuel ratio
OFDF	opposed-flow diffusion flame
PDE	partial differential equation
PETTT	productivity enhancement, technology transfer, and training
PSB	Propulsion Science Branch
SD	San Diego
SFRJ	solid-fuel ramjet
TMM	trial mechanism method

1 (PDF) DEFENSE TECHNICAL INFORMATION CTR
DTIC OCA

1 (PDF) CCDC ARL
FCDD RLD CL
TECH LIB

1 (PDF) CCDC ARL
FCDD RLW LD
M MCQUAID

2 (PDF) CCDC AVMC
RDMR WDP P
M PFEIL
RDMR SSM A
M VAUGHN

3 (PDF) NAWCWD-CHINA LAKE
E WASHBURN
B BOJKO
C DENNIS

2 (PDF) NSWC-INDIAN HEAD
H HAYDEN
T HEDMAN

6 (PDF) NRL
B FISHER
R JOHNSON
T LOEGEL
A EPSHTEYN
G GOODWIN
D KESSLER

1 (PDF) ONR
C STOLZ

1 (PDF) AFRL MUNITIONS
S PEIRIS

1 (PDF) USAF
V SANKARAN

22 (PDF) CCDC ARL
FCDD RLR EN
5 (HC) R ANTHENIEN
FCDD RLR PC
J PARKER
FCDD RLV P
L BRAVO ROBLES
FCDD RLW L
T SHEPPARD
FCDD RLW LB
J BRENNAN
E BYRD
FCDD RLW LD
C CHEN
JD VEALS
MJ MCQUAID (1 PDF, 5 HC)
MJ NUSCA
S ISERT
A MCBAIN
A WILLIAMS
J COLBURN
FCDD RLW LH
M MINNICINO
A RAWLETT
J CIEZAK-JENKINS

1 (PDF) EMBRY-RIDDLE AEORNAUTICAL UNIV
S MARTIN

1 (PDF) REACTION SYSTEMS, INC.
B HITCH

3 (PDF) PURDUE UNIV
S SON S
T POURPOINT
C GOLDENSTEIN

1 (PDF) UCSD UNIV
K SESHADRI

1 (PDF) MIT UNIV
W GREEN

1 (PDF) ARGONNE NATL LAB
S KLIPPENSTEIN

1 (PDF) STANFORD UNIV
I BATTIATO

1 (PDF) PALO ALTO RESEARCH CTR
M BEHANDISH

3 (PDF) DARPA
K MASSARO
J VANDENBRANDE
G HARABIN